POSTPRINT ACCEPTED

ESPL WILEY

Geodynamic control on Pleistocene coral reef development: Insights from northwest Sumba Island (Indonesia)

Gino De Gelder[1,2] | Tubagus Solihuddin[1] | Dwi Amanda Utami[1] |
Marfasran Hendrizan[1] | Rima Rachmayani[3] | Denovan Chauveau[4] |
Christine Authemayou[5] | Laurent Husson[2] | Sri Yudawati Cahyarini[1]

[1]Paleoclimate & Paleoenvironment Research Group, National Research and Innovation Agency (BRIN), Bandung, Indonesia

[2]ISTerre, CNRS, IRD, Univ. Grenoble Alpes, Grenoble, France

[3]Oceanography Research Group, Faculty of Earth Sciences and Technology, Bandung Institute of Technology, Bandung, Indonesia

[4]Dipartimento di Scienze Ambientali, Informatica e Statistica (DAIS), Ca' Foscari University of Venice, Venice, Italy

[5]LGO, IUEM, CNRS, UMR 6538, Université de Bretagne Occidentale, Plouzané, France

Correspondence
Gino De Gelder, ISTerre, CNRS, IRD, Univ. Grenoble Alpes, Grenoble, France.
Email: ginodegelder@gmail.com

Abstract

The fossil record of Quaternary reef systems, as expressed in uplifted regions by sequences of stacked terraces, has been extensively used either to understand their morphodynamics or to unravel sea level variations. Yet, because these two aspects are intimately linked, Quaternary reef analysis is often underdetermined because the analysis often focuses on single sequences, along one-dimensional profiles. Here, we take advantage of the lateral variations of coral reef sequences by documenting the morphological variations of the reef sequence on Sumba Island. Near Tambolaka, northwest Sumba, we analysed a reef transect, topography, and associated sedimentological record to obtain a precise coral reef stratigraphy and geomorphic patterns that can be compared with the well-documented eastern counterpart. In Tambolaka, the reef sequence displays four lower layers of bedded chalky limestone units with a weakly cemented sandy matrix, which we attribute to the Middle Miocene to Pliocene Wakabukak formation based on calcareous nannofossils and planktonic foraminifers. The uppermost layer is a calcretized reefal limestone unit with a well-lithified sandy matrix, which we attribute to the Plio–Pleistocene reef sequence of the Kalianga formation. Seven marine terraces imprint the regional morphology, four of which we correlate with Marine Isotope Stage (MIS) 5e, MIS 7e, MIS 9e, and MIS 11c terraces of Cape Laundi, northeast Sumba. When scrutinized at the light of numerical models of reef development, these results indicate that the morphodynamics of reefal sequences is strongly impacted by the tectonic evolution. The geodynamic context sets both the extrinsic conditions of reef development, such as the morphology of the basement and hydrodynamics, and the intrinsic properties, in particular reef growth rate. While the morphodynamic evolution of the sequence is at first-order representative of the interplay between uplift rates and sea level oscillations, the detailed assemblage of the reef units drastically varies along the coastline.

KEYWORDS
coral reefs, marine terraces, northwest Sumba, sea level, tectonics, uplift

1 | INTRODUCTION

Studies of coral reef terrace sequences provide crucial clues about past sea levels and tectonic activity (e.g., Bard et al., 1996; Chappell, 1974; Taylor & Mann, 1991). As living coral reefs adjust to relative sea level variations, their fossilized counterparts act as geomorphic and biological markers of past relative sea levels. Due to their extent, preservation, and datable material, some coral reef terrace sequences, such as Barbados (Fairbanks, 1989; Peltier & Fairbanks, 2006), Huon in Papua New Guinea (Chappell & Polach, 1991; De Gelder et al., 2022), and Sumba in Indonesia (Bard et al., 1996; Pirazzoli et al., 1991, 1993), have received much more attention than others. In all of these locations, most studies have been dedicated to a few key profiles: the reef sections in Barbados (Fairbanks, 1989; Peltier & Fairbanks, 2006), the Bobongora, Kanzarua, and Sialum sections in Huon (Chappell & Polach, 1991; De Gelder et al., 2022), and the Cape Laundi section in Sumba (Chauveau, Authemayou, Pedoja, et al., 2021; Hantoro, 1992; Pirazzoli et al., 1991, 1993).

Numerical geomorphic analysis of high-resolution digital elevation models together with numerical models of coral reef growth has provided a breakthrough in understanding the links between sea level changes and the morphological record of coastlines (e.g., Koelling et al., 2009; Leclerc & Feuillet, 2019; Toomey et al., 2013). Especially for Huon, it has been demonstrated that it is worthwhile to consider the lateral variations in terrace elevations, ages, and uplift rates, to better constrain paleo sea level and tectonic processes (De Gelder et al., 2022). On Sumba Island, although several studies have pointed out the lateral changes in terrace elevations (Authemayou et al., 2018, 2022; Nexer et al., 2015), little is known about the coral reef terraces outside of the Cape Laundi profile. In this study, we aim to fill that gap, by exploring geologic and geomorphic lateral variations between Cape Laundi and the coral reef terraces ∼100 km westward.

Sumba Island is part of the Lesser Sunda Islands Group comprising mainly the islands of Bali–Lombok–Sumbawa–Flores–Alor–Wetar. The island is interpreted as a microcontinent from Sundaland that moved to its current position ∼20 Ma (Early Miocene), when the islands group of Lesser Sunda had not yet been formed (Abdullah et al., 2000; Burollet & Salle, 1981; Hamilton, 1979; Satyana & Purwaningsih, 2011a; Soeria-Atmadja et al., 1998). The regional tectonic setting has determined much of the contemporary landforms and controlled the development of the uplifted landscapes by which Quaternary reef systems have emerged (Bard et al., 1996; Jouannic et al., 1988; Pirazzoli et al., 1991, 1993).

Quaternary reefs in Sumba Island have developed over the Tertiary (Mio–Pliocene) limestones of the Waikabubak Formation in the western part and marly sandstones of the Kananggar Formation in the eastern part, forming major geomorphic features for over 300 km across the island. While the reef systems in northeast Sumba have been well-studied, especially at Cape Laundi (Chauveau, Authemayou, Molliex, et al., 2021; Chauveau, Authemayou, Pedoja, et al., 2021; Pirazzoli et al., 1991, 1993), the reef systems in northwest Sumba are relatively poorly recognized and understudied. Yet, the morphology of the Quaternary reefs profoundly varies along-strike, and it is still unclear how the well-identified geomorphic patterns from the Quaternary reefs of east Sumba correlate to the coral reef sequence of west Sumba or how they have developed as distinctive morphologies driven by different tectonic settings.

A comprehensive study from Nexer et al. (2015) demonstrated morphometric indices of catchment areas across the Quaternary reefal limestone of Sumba Island to derive coastal uplift rates based on analysis of Cape Laundi coral reef terrace IIIb, which they correlated with the Marine Isotope Stage (MIS) 11. More recently, Chauveau, Authemayou, Pedoja, et al. (2021) revisited the chronology of the Cape Laundi sequence through an integrated approach combining ^{36}Cl cosmogenic concentrations and ^{230}Th/U ages. Chauveau, Authemayou, Molliex, et al. (2021) characterized the dynamics of coastal drainage in Cape Laundi based on high-resolution topographic data, geomorphological analysis, and denudation rates derived from ^{36}Cl cosmogenic nuclide concentrations. Authemayou et al. (2018) underlined the role of normal faults as the main driving force in the drainage rearrangement of west Sumba in addition to asymmetric uplift and groundwater flow. Authemayou et al. (2022) used structural data, marine terrace analysis, drainage evolution, and focal mechanisms around Sumba to show that the island is affected by dextral en echelon folding triggered by subduction of the western lateral boundary of the Australian continental margin. However, no comprehensive chronological framework has yet been proposed in a previous study for the northwest Sumba coral reef terraces.

This study focuses on a reef transect to assess the reef lithostratigraphy within the exposed mine pit of Tambolaka, northwest Sumba. The outcrop enables detailed stratigraphic, paleoecological, and geochronological analyses spanning the entire reef growth history. Furthermore, we present a detailed geologic/geomorphic comparison between Tambolaka in northwest Sumba and Cape Laundi in northeast Sumba, using a combination of geomorphic indices and numerical reef modelling. This integration allows us to address features like reef geochronology, accretion history, and uplift rates of northwest Sumba. Thus, the primary aim of this paper is to obtain (1) a better understanding of reef lithostratigraphy in northwest Sumba through a reef transect within the exposed mine pit of Tambolaka, (2) lateral variations including terrace elevations, ages, and uplift rates between Cape Laundi northeast Sumba and Tambolaka northwest Sumba through a detailed analysis of changes in geomorphology, and (3) geomorphic patterns and potential growth of reef sequences in west Sumba through numerical reef modelling. Because geometry, composition, and evolution of coral reef systems provide important geological estimates of past relative sea levels and tectonic motions (Camoin & Webster, 2015), this paper provides a basic framework for considering past and future modes of reef response to sea level and tectonic changes at various timescales.

2 | BACKGROUND

2.1 | Geological setting

Sumba Island is part of the Wallacea region, a transitional area between Asiatic fauna groups in the west and Australia in the east, characterized by a high level of endemicity and local specific faunas (Satyana & Purwaningsih, 2011b). Based on rock characteristics, fossil composition, and gravity analysis, it is thought that Sumba Island was probably once part of Sundaland and drifted southwards by back-arc spreading from South Sulawesi to its current position in the Early Miocene (Hall, 2002; Hall & Smyth, 2008; Rangin et al., 1990;

Rutherford et al., 2001; Satyana & Purwaningsih, 2011a; Wensink & van Bergen, 1995). During the Late Miocene, thick buoyant continental Australian crust subducted under the Banda arc, causing the Sumba ridge to rise and emerge (Fortuin et al., 1997; Haig, 2012; Hall & Smyth, 2008; Harris, 1991; Tate et al., 2014). This rise resulted in (1) the diachronic emergence of Sumba ridge 3 Ma years ago in the east and 1 Ma years ago at Cape Laundi (Pirazzoli et al., 1993), (2) the formation of Quaternary coral reef terraces on the northern flank, and (3) a coeval south-verging collapse of the southern flank (Authemayou et al., 2018; Fleury et al., 2009).

Sumba Island tectonically lies at the plate boundary and transitions from oceanic subduction in the west to island arc–continent collision in the east. To the west, the oceanic crust of the Indo-Australian plate subducts beneath the Sunda arc at the Java Trench (Figure 1). To the east, conversely, the Australian continental crust has been underthrusting the Banda arc at the Timor Trough since the Late Miocene. This underthrusting event remodelled subduction dynamics and profoundly reshaped the entire morphotectonic pattern of the

region, as it triggered the pervasive subsidence of the Sunda Shelf in the West and the Sahul Shelf in the Southeast while uplifting Wallacea in between (Husson et al., 2022) and the islands Flores, Timor, and Sumba in particular (e.g., Zhang & Miller, 2021), where it formed a collision zone (Authemayou et al., 2022; Bock et al., 2003; Hall, 2002, 2012; Harris, 2011; Nugroho et al., 2009; Pacheco et al., 1993; Satyana & Purwaningsih, 2011a; Simons et al., 2007; Spakman & Hall, 2010). Consequently, two trench systems border southern Sumba Island (Satyana & Purwaningsih, 2011b). First, the 6 km deep Java Trench—associated with the Sunda Arc—is located south of Bali and Sumbawa, where the oceanic lithosphere of the Indo-Australian plate subducts below Sundaland. Second, the 3 km deep Timor Trough stretches from the south of Sumba Island towards the northeast, where the continental lithosphere of the Indo-Australian plate subducts beneath Timor, Tanimbar, and some smaller islands (Figure 1; Satyana & Purwaningsih, 2011b). The subduction of the Indo-Australian plate in the Java Trench has formed the active volcanic islands of Bali, Lombok, Sumbawa, Flores, and some smaller islands.
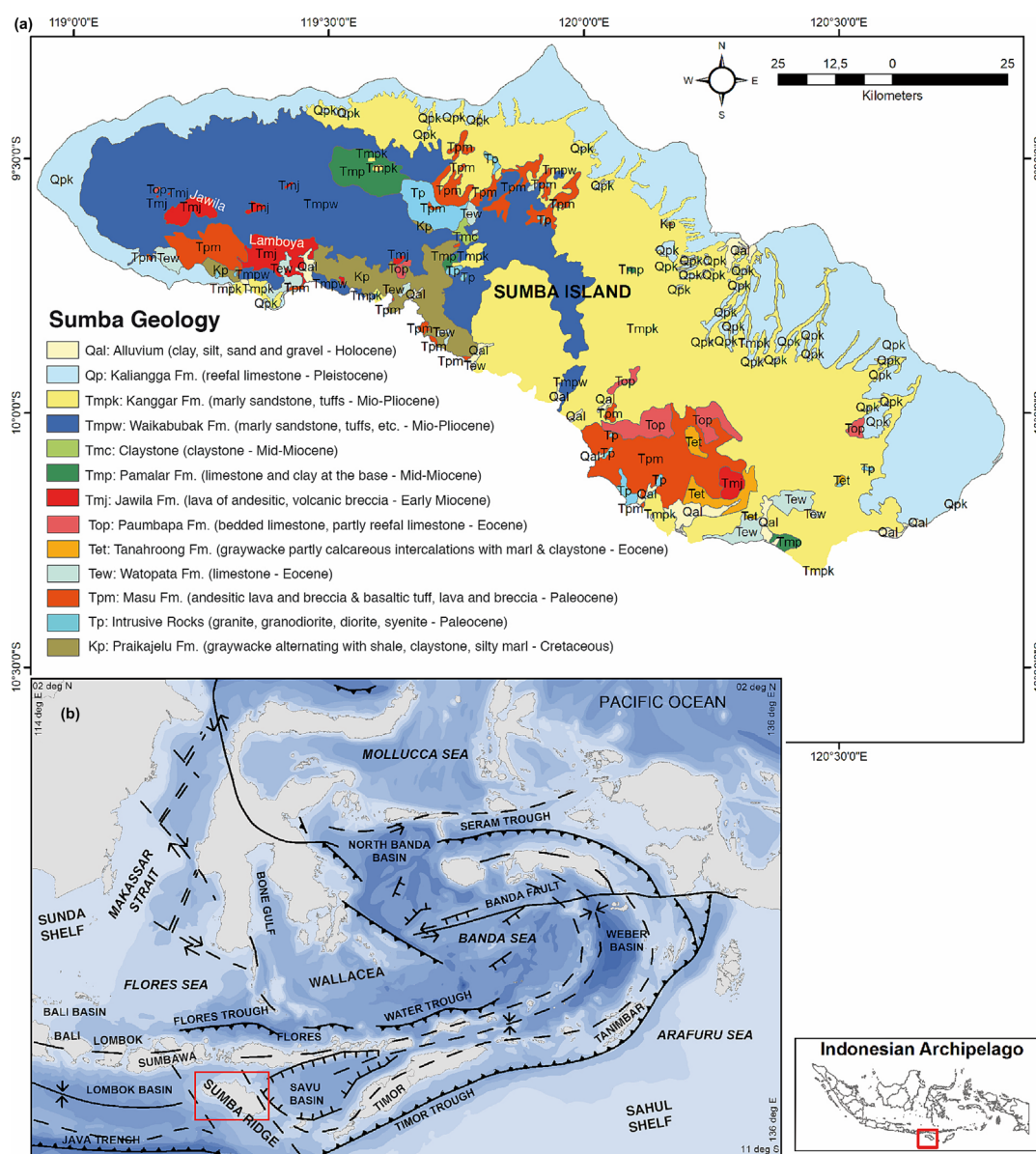
FIGURE 1 Geological map and tectonic setting of Sumba Island. (a) Geological map of Sumba Island (after Effendi & Apandi, 1993) and (b) Sumba Island in the regional tectonic setting of eastern Indonesia (after Abdullah et al., 2000; Burollet & Salle, 1981; Hamilton, 1979).

2.2 | Stratigraphy

The oldest rock exposed on Sumba Island (Figure 1) on the southern coast of Sumba is the Praikajelu Formation. This formation is composed of Late Cretaceous greywacke, shale, clay, stone, silty marl, and clayey sandstone. During the Paleocene, two significant magmatic periods formed the lavas and andesitic breccias of the Masu Formation and intrusive rocks (granite, granodiorite, diorite, and syenite). Overlying these are the Eocene limestones of the Watopata Formation interfingering with the partly calcareous greywacke of Tanahroong Formation. Following this, the Paumbapa Formation consists of partly reefal limestones that were unconformably deposited during the Oligocene. The mid-Miocene claystones of the Pamalar Formation were deposited in an unconformity (Effendi & Apandi, 1993).

On the western side, the Mio–Pliocene rocks are composed of widespread transgressive carbonate series of the Waikabubak Formation consisting of limestones, clayey limestones, and tuffaceous marls. On the eastern side, the turbiditic chalky sediments of Kananggar Formation consist of marly sandstones, tuffaceous sandstones, tuffs, sandy marls, and limestones. The Neogene was marked by syn-sedimentary tectonics, evidenced by normal faulting and large-scale slumping (Authemayou et al., 2018). The Quaternary rocks are reefal limestones of the Kaliangga Formation overlay the Waikabubak and Kananggar Formations. Recent alluviums are composed of clays, silts, sands, and gravels (Astjario, 2006; Effendi & Apandi, 1993).

3 | METHODOLOGY AND METHODS

3.1 | Mapping

The land topography data covering the study area are derived from a DEMNAS Digital Elevation Model (http://tides.big.go.id/DEMNAS) with a spatial resolution of 0.27 arc-sec of longitude and latitude and referenced to the Earth Gravitational Model 2008 for the vertical datum. The spatial and vertical resolutions of the DEM are 8 and 1.8 m, respectively. The DEM combines elevation data from IFSAR/TERRASAR-X and ALOS PALSAR, with spatial resolutions of 5 and 11.25 m, respectively, in addition to mass point data resulting from stereo-plotting. For the ocean bathymetry, we used BATNAS data (https://tanahair.indonesia.go.id/demnas/#/batnas). These bathymetric data were acquired within an offshore survey from the Center for Marine and Coastal Environment, the Geospatial Information Agency of the Republic of Indonesia. It has largely been generated from a database with interpolation between soundings guided by satellite-derived gravity data. From the data source, it is not clear what is the spacing between soundings in specific areas, like the area we analysed offshore Sumba, so we emphasize that these data should mainly be seen as first-order approximations of the bathymetry. The spatial resolution of BATNAS data is 6 arc-sec of latitude and longitude in relation to the mean sea-level datum (∼180 m resolution around Sumba), whereas there are no robust estimates of the vertical uncertainty.

We used these elevation data to systematically map the sequence of the reef terraces on slope maps and elevation maps. The landward limit of Quaternary reefal terraces on the large-scale map (Figure 2a) was based on the morphologic contrast in roughness between the relatively smooth Quaternary terraces and relatively high-relief older formations and corroborated with the geological map (Figure 1). The seaward limit of the Quaternary reefal terraces was approximated by the 130 m bathymetric isobath. This number approximately corresponds to the sea level depth during the Last Glacial Maximum (∼20 ka), which should be indicative of the lowermost limit of Quaternary terraces in uplifting areas like Sumba. The reef terrace mapping of the Cape Laundi terraces is based on Chauveau, Authemayou, Pedoja, et al. (2021), whereas the reef mapping of the Tambolaka section is based on a lateral correlation of reef terraces and morphological observations. Near-shore bathymetric estimates were obtained through a diving expedition offshore the main Tambolaka profile (Figure 2b), with depths approximated based on height of the divers (∼0.5 m uncertainty) and first-order width based on handheld GPS (few metres uncertainty).

3.2 | Stratigraphic log and fossil analysis

A reef transect was established to log the sedimentary exposures in the Tambolaka open-cut pit, and the transect line was selected along with the workable exposure. Using DEMNAS DEM, we estimated the base of the pit at 8 ± 2 m above sea level (masl). A vertical transect from the base to the top (∼23 m high, so between 8 and 31 masl) was logged, sampled, and photographed to obtain information including (1) the ratio of coral clasts and matrix (following Embry & Klovan, 1971); (2) sediment textural characteristics (using the Udden–Wentworth nomenclature and a visual assessment of sediment composition); and (3) preliminary coral generic identification. Reef framework analysis and facies descriptions, following Montaggioni (2005), highlight the growth forms of the dominant coral reef builders and key environmental indicators. Position fixing uses a built-in GPS and camera on a smartphone.

Rock samples for fossil analysis were collected from a subset of transects on every reef sequence. At each sampling site, 1 kg of rock samples was collected for planktonic foraminifera identification as necessary. All samples were washed through a 63 μm sieve and dried at 40°C temperature overnight. The residue from a gram of samples was examined using the binocular microscope Olympus SZX40 and the portable scanning electron microscope Phenom ProX Thermo fourth generation at the Research Center for Climate and Atmosphere of BRIN. Foraminifera and calcareous nannofossils are identified based on a previous study by Bolli et al. (1985).

3.3 | Geomorphological analysis

To have a detailed understanding of lateral variability in geomorphic characteristics of the N-Sumba coast, we assessed coral reef terrace elevations, present-day reef widths, offshore reefal terrace widths, and offshore slopes between Cape Laundi and Tambolaka. To assess coral reef terrace elevations, we used stacked swaths (Armijo et al., 2015; Fernández-Blanco et al., 2020), which is a combined plot of hundreds of parallel topographic profiles that can aid in understanding lateral coral reef terrace correlations (De Gelder et al., 2022). To obtain a good balance between readability and detail, we opted for 900 parallel profiles of 20 m width, using average elevation
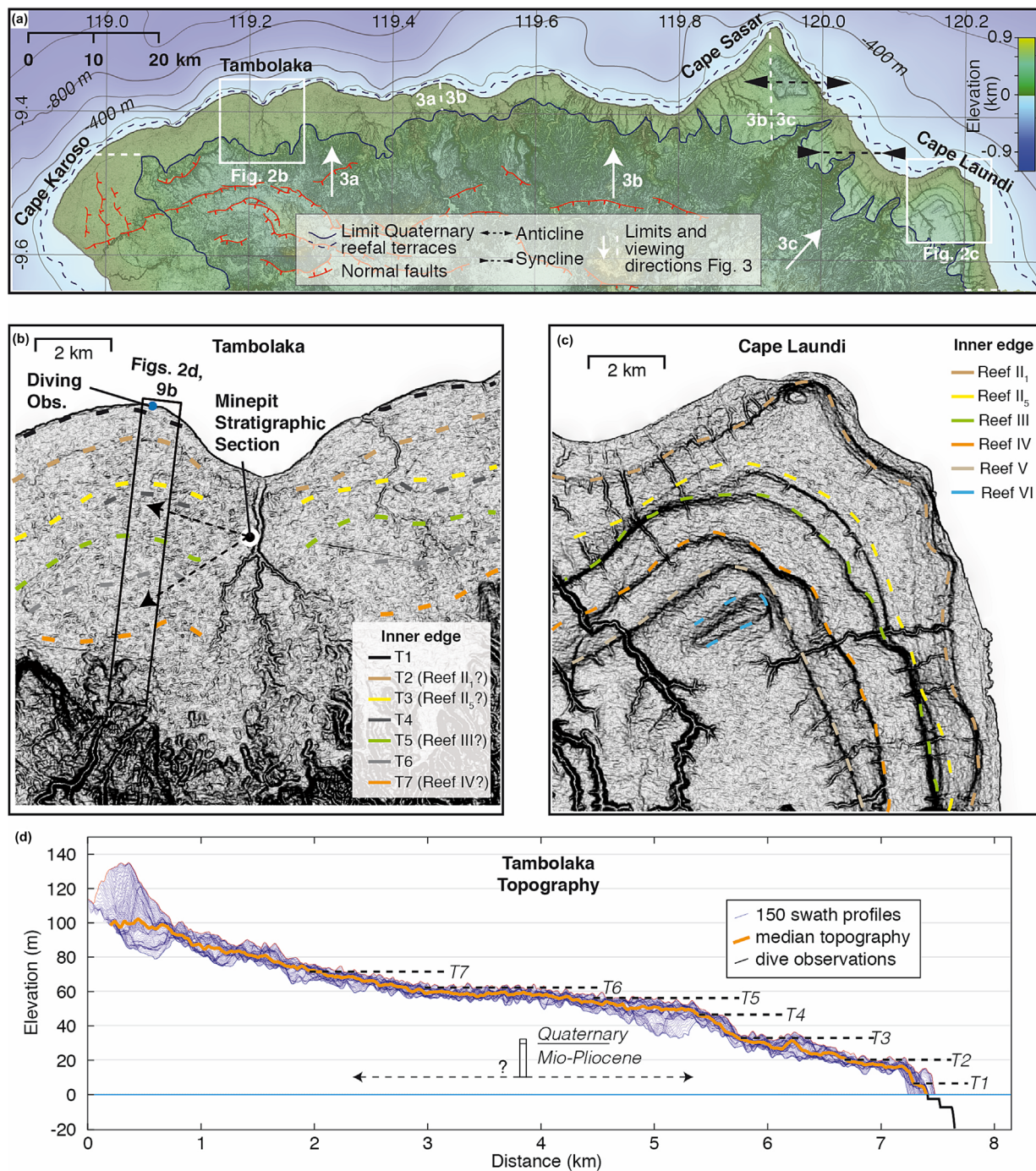
FIGURE 2 Coral reef terraces between Cape Laundi and Tambolaka. (a) Slope map of the northwest Sumba coastal area studied here, overlain with coloured elevations. Limits of Quaternary reefal terraces were drawn from the BATNAS bathymetry and DEMNAS topography (see Section 3), whereas normal faults and folds are redrawn from Authemayou et al. (2022). (b) Slope map of the Tambolaka area, with the location of the stratigraphic section analysed here and seven mapped coral reef terrace levels. (c) Slope map of Cape Laundi area, with reef labels and inner edges from Chauveau, Authemayou, Pedoja, et al. (2021). (d) Stacked swath profile of the Tambolaka coral reef terrace sequence, with its location given in (b), and bathymetric observations made by diving in the shallow reef areas offshore. Below the stacked swath profile, we show the possible location of our stratigraphic section when translated from its location near the river to this cross-section.

measurements for every 50 m along the profile. For the area between Tambolaka and Cape Sasar, we used a northward viewing angle (Figure 2a) and, for the area between Cape Sasar and Cape Laundi, a northeastward viewing angle (N041E; Figure 2a), in both cases roughly parallel to the present-day coastline. We limited this analysis to the topography of onshore Quaternary reefal terraces. For the lateral correlation of reef elevations, we used the same reef nomenclature as in Chauveau et al. (2023) at Cape Laundi and assessed the

continuity of the terraces westward for the inner edges of four reefs (Reefs II_1, II_5, III, and IV), both using the stacked swath profiles and in map view. We selected these reef units as reference datum, as ages (Bard et al., 1996; Pirazzoli et al., 1993) and modelling (Chauveau et al., 2023) suggest that they emerged during the four most recent major interglacial highstands: MIS 5e (~125 ka), MIS 7e (~240 ka), MIS 9e (~325 ka), and MIS 11c (~400 ka). As sea level elevations during these highstands were relatively high, the corresponding terraces

can be expected to be currently exposed above sea level even for relatively low uplift rates (De Gelder et al., 2022; Pastier et al., 2019).

To better understand if there is a link between long-term (∼400 ka) reef formation processes and the formation of the present-day reef, we calculated the present-day reef width based on historical imagery from Google Earth. Specifically, we used available images from 2003 to 2022, consisting of Landsat, Sentinel, and Maxar satellite images with resolutions of ∼30 cm to 15 m. We based our mapping on the contrast between lighter (shallow) offshore portions and darker (deeper) offshore portions. We emphasize that this mapping strategy is ambiguous at some locations where images are not clear and should thus be taken as first-order width estimates with uncertainties on the order of some tens of metres. To attribute more confidence to our mapping, we verified our mapping with the Allen Coral Atlas (2022) every 5 km. This atlas used 10 m resolution Sentinel-2 surface reflectance data, taking the median bathymetry calculated over 12 months, down to a depth of 15 m below mean sea level. The kml file of our reef mapping is given as Data S1. We marked the reef edge roughly every 150 m along the coastline, wherever it was clearly visible from the imagery. We did the same for the present-day coastline and used linear interpolation for both the present-day coastline and reef edge to have measurements exactly every 150 m. As for the stacked swaths, we used an N–S orientation to calculate the reef width between Tambolaka and Cape Sasar and an NE–SW (N041E) orientation for the reef between Cape Sasar and Cape Laundi. We corrected for the local orientation of the coastline to approximate the width perpendicular to the coastline, using the following equation for the interval between Tambolaka and Cape Sasar:

$$PRW_i = ORW_i \cdot \cos\left(\tan^{-1} \frac{|y_{i-1} - y_{i+1}|}{|x_{i-1} - x_{i+1}|}\right), \tag{1}$$

in which PRW is the perpendicular reef width, ORW the oblique reef width, y_{i-1} and x_{i-1} the coordinates in m (based on Universal Transverse Mercator projection) for the measurement 150 m to the west, and y_{i+1} and x_{i+1} for the measurement 150 m to the east. For the section between Cape Sasar and Cape Laundi, we applied the same equation but after rotating both the coastline and reef edge by 41° counterclockwise. For all the resulting reef width estimates, we applied a 5 km moving average to filter out short wavelength variations in relation to small river outlets.

To calculate the offshore reefal terrace width, we used the same procedure as Equation (1) but measured the difference between the present-day coastline and the −130 m depth contour (Figure 2a) instead. To calculate the offshore slope as a percentage, we also used the same procedure as Equation (1) but estimated the horizontal distance between the −130 and −200 m contour (Figure 2a) and the horizontal distance between the −130 and −400 m contour (Figure 2a) instead. We then divided 70 and 270 m, respectively, by those distances.

3.4 | Reef modelling

Landscape evolution models provide a way to evaluate the full geometry of a marine terrace sequence, not just the elevation of a terrace, and help distinguish the most likely chronology (e.g., De Gelder

et al., 2020; Leclerc & Feuillet, 2019; Toomey et al., 2013). To reproduce the coral reef terrace sequence at Tambolaka and evaluate to what extent the controlling parameters vary between Cape Laundi and Tambolaka, we use the REEF code (see details in Husson et al., 2018; Pastier et al., 2019). This is a kinematic profile evolution model that takes into account vertical land motion, reef growth, marine erosion, and the deposition of the eroded clastic sediments, acting on an initially linear slope. Reef growth is defined through a potential reef growth rate, consisting of a vertical component and a horizontal component. The vertical component of aggradation accounts for the decreasing coral growth rate with increasing depth as a response to light attenuation, whereas the horizontal component of progradation accounts for the decreasing coral growth from the reef crest (facing the open sea) towards the shore. Marine erosion is based on the wave erosion model of Anderson et al. (1999), consisting of a vertical seabed erosion component and a horizontal cliff erosion component. In this model, these are approximated by an eroded volume, in which the proportions between vertical and horizontal erosions rely on wave dissipation (Anderson et al., 1999). Clastic sediment deposition takes into account the eroded rock volume, in which horizontal deposition occurs in lagoons, and at a repose angle of 10% at the base of the forereef slope.

We selected a topographic profile ∼2 km west of the Tambolaka River (Figure 2b), which may have caused anomalous sedimentation and erosion patterns during the development of the reefal sequence (at short distances from the stream) but may have also remodelled the landscape during subaerial exposure following uplift (detailed topography in Figure S1). The slope of this profile is between 1% and 2%, which we both tested as input parameters. We tested uplift rates of 0.125, 0.15, and 0.175 mm/year, as the reef elevations at Tambolaka are approximately between one third and one fourth of the elevations at Cape Laundi, which are thought to be uplifting at rates of ∼0.5 mm/year (Chauveau et al., 2023). We used potential reef growth rates between 1 and 6 mm/year, the former being the minimum value in the REEF model and the latter the best-fitting reef growth rate for Cape Laundi (Chauveau et al., 2023). For eroded volumes, we tested 60 mm³/year (as in Chauveau et al., 2023), as well as higher values of 180 and 360 mm³/year given the generally higher wave energy in Tambolaka compared with Cape Laundi (see Wavewatch data from Tolman, 2009 in Nienhuis, 2019). We ran the models for 1 Ma and tested four different sea level curves that were derived with different methodologies: (1) the sea level curve of Waelbroeck et al. (2002) derived from a composite δ¹⁸O curve that was corrected with a global coral data compilation, (2) the curve of Bintanja et al. (2005) derived through inverse ice-sheet modelling, (3) the curve of Grant et al. (2014) derived from a synchronization of an Asian monsoon record with a hydraulic control model of the Red Sea Basin (Rohling et al., 2009), and (4) the curve of Spratt and Lisiecki (2016) derived from a principal component analysis of seven other sea level curves. Only one of these curves spanning 1 Ma is the curve of Bintanja et al. (2005), so we added the sea level elevations of Bintanja et al. (2005) for the intervals that are absent in the other curves: 450–1000 ka for Waelbroeck et al. (2002), 500–1000 ka for Grant et al. (2014), and 800–1000 ka for Spratt and Lisiecki (2016). The maximum and optimum reef growth depth are set to 20 and 2 m depth, respectively (based on Bosscher & Schlager, 1992), and the wave base at 3 m depth based on field observations.

4 | RESULTS

4.1 | Stratigraphy and paleoecology

Stratigraphic and paleoecological data from the measured reef section of Tambolaka can be summarized as follows (Figure 3): The lowermost section of the open-cut pit is a bedded chalky limestone unit (up to ∼7 m thick) with a sandy matrix. The rock mainly contains recrystallized corals and a weakly cemented, pale yellow, fine to coarse grain-sized sandy matrix. This unit mainly consists of domal corals with a diameter no larger than 30 cm. Faviidae are predominant including Cyphastrea, Platygyra, Diploastrea, Uolophyllia, and Leptastrea spp. (Figure 4). Overlying this, a two-bedded chalky limestone unit (∼5 m thick each) contains crystalline arborescent and domal coral fragments in a weakly cemented, pale grey, fine to coarse-grained sandy matrix. Coral colonies are generally small, difficult to identify, and invariably recrystallized. Above this unit is a brownish-chalky limestone (up to ∼5 m thick) with a fine to coarse-grained sandy matrix. Coral colonies are dominated by Poritidae including Goniopora and Porites spp. but also contain colonies from the genera of Merulinidae such as Hydnophora sp (Figure 4). Coral colonies are typically small, approximately 10–30 cm in diameter. All stratigraphic sections of the bedded chalky limestone are matrix-supported and classified as floatstone reef facies with abundant and diverse molluscan fauna.

A calcretized reefal limestone unit of 1 to 1.5 m of thickness is found at 30 masl, in the uppermost portion of the reef sequences in the measured section profile. This is a minimum thickness because the top of this unit is eroded, and it may thus be thicker elsewhere (Figure 3). The rock primarily contains coralline algae with minor coral. Coral fragments are mostly crystallized in a well-cemented, dark grey, fine to coarse-grained sandy matrix. Shell fragments, sea urchins, and gastropods are abundant. The coral clasts are visually well-coated with encrusted algae.

The measured section of the Tambolaka mine pit contains rare and well-preserved foraminifera and calcareous nannofossil assemblages. Planktonic foraminifera in this limestone unit consists of *Globorotalia opima opima*, *Globorotalia tumida*, *Globorotalia pertenuis*, *Globorotalia pseudomiocenica*, and *Globorotalia plesiotumida* (Figure 5). These foraminifera assemblages indicate a wide age range between

Legend:

- calcretized reefal limestone with recrystalized corals and encrusting coralline algae
- Bedded chalky limestone unit with brownish fine to coarse-grained sandy matrix
- Bedded chalky limestone unit with pale grey, fine to coarse-grained sandy matrix
- Bedded chalky limestone unit containing recrystalized coral s in a pale yellow, fine to coarse -grained sandy matrix

FIGURE 3 Lithostratigraphic summary of the measured reef section. Section of Tambolaka mine pit showing at least five different reef assemblages. Elevation of the base of the section is based on DEM and Google Earth analysis (see Section 3) and elevations upwards based on tape measurements.
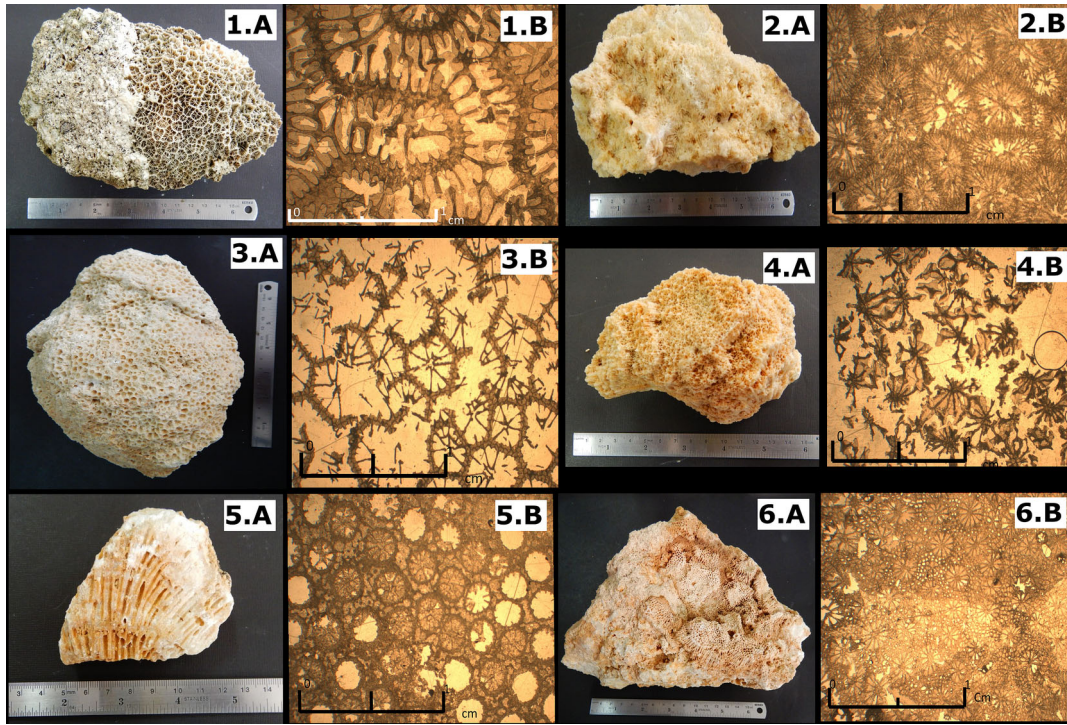
FIGURE 4 Coral colonies of the bedded chalky limestone units of the Tambolaka mine pit. Corals were identified from the lowermost layer and the fourth layer of the measured reef sequences. Letter A indicates coral colonies and B shows thin sections of the coral colonies. The coral colonies are (1) Platygyra sp, (2) Diploastrea sp, (3) Leptastrea sp, (4) Hydnophora sp, (5) Goniopora sp, and (6) Porites sp.
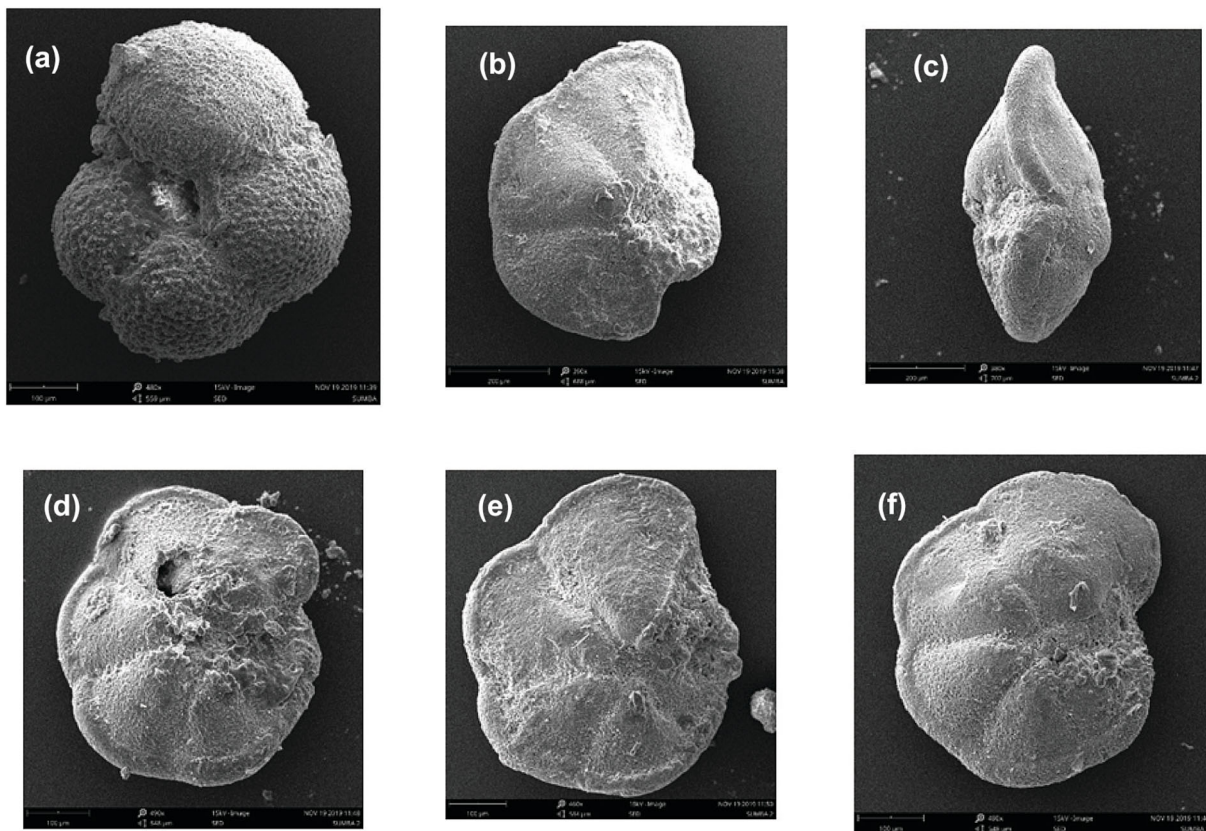
FIGURE 5 Planktonic foraminifera assemblages in a bedded chalky unit. (a) *Globorotalia opima opima*, (b) *Globorotalia tumida*, (c) *G. tumida*, (d) *Globorotalia pertenuis*, (e) *Globorotalia pseudomiocenica*, and (f) *Globorotalia plesiotumida*.

the Oligocene and Pliocene. Besides foraminifera, calcareous nannofossils are identified in a bedded chalky limestone unit at the bottom of the unit (Figure 6). Several genera of calcareous nannofossil identified in that layer are *Calcidiscus*, *Helicosphaera*, *Coccolithus*, *Discoaster*, *Umbilicosphaera*, and *Reticulofenestra*. The relative ages of the strata, based on analysis of calcareous nannofossils, range from Middle Miocene to Pliocene in the lowermost bedded chalky limestone, based on the presence of both *Umbilicosphaera sibogae* (Middle Miocene–Pleistocene) and *Calcidiscus macintyrei* (Early Miocene–Pliocene) in the same assemblage (Figure 6). One species of *Discoaster mohleri* was found in the fossil reef deposit of the Tambolaka mine pit, suggesting a Paleocene age. However, we believe this nannofossil has been reworked from an older formation.

Based on the fossil record, we conclude that the sequence is mostly Middle Miocene to Pliocene in age, which we assign to the Waikabukak formation (Figure 1). The lithology indicates that the Pleistocene to recent Kalianga formation there is only represented by the topmost unit that clearly display the typical facies of a fossil coral reef unit.

4.2 | Reef morphology

The reefal limestones of the Kalianga Formation mostly appear in North Sumba; they were formed as carbonate series and were uplifted to form sequences of coral reef terraces, representing major geomorphic features along the coast (Figure 2a; Authemayou et al., 2022; Chauveau, Authemayou, Pedoja, et al., 2021; Chauveau et al., 2023; Effendi & Apandi, 1993; Nexer et al., 2015; Satyana & Purwaningsih, 2011b). In Tambolaka and the surrounding area, we identified seven reef terraces in the field and from the DEM data (Table 1 and Figure 2b; uninterpreted version of this map in Figure S1) and correlate them to the well-described sequence of Eastern Sumba (Figure 7; uninterpreted version of this figure in Figure S2). The lower terrace T1 is developed at an elevation of ~8–10 m, is up to 200 m wide, and stretches along the coast of northwest Sumba forming steep rocky cliffs. The second terrace T2 is developed at a height of ~18–20 m with a width of at least 400 m. Based on our lateral correlation of terraces (Figure 7), we propose this terrace as the equivalent of terrace II_1 (±60 m high;
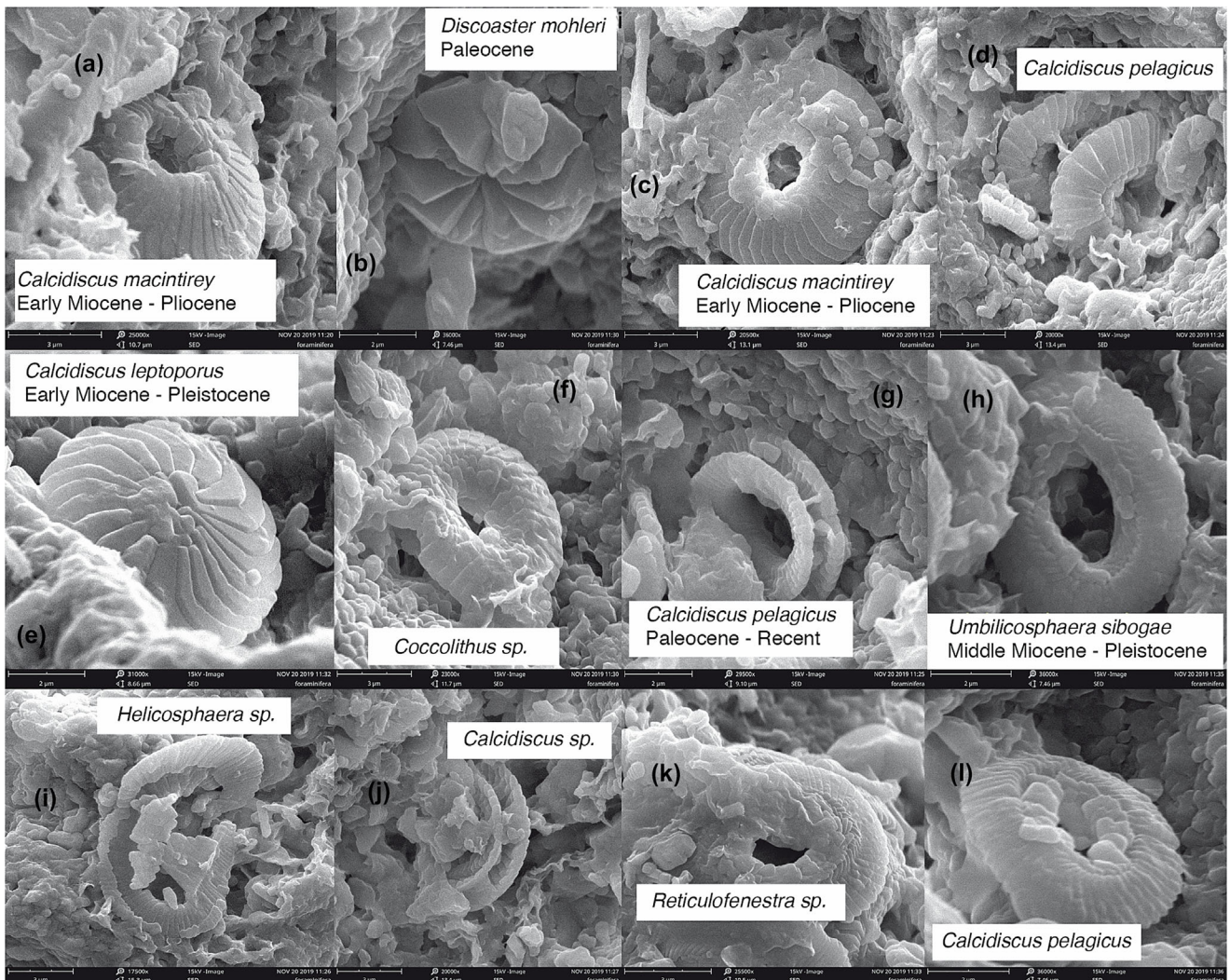
FIGURE 6 Calcareous nannofossil assemblages. Analysed from the lowermost bedded chalky limestone. (a) *Calcidiscus macintirey* (Early Miocene to Pliocene), (b) *Discoaster mohleri* (Paleocene), (c) *Calcidiscus macintirey* (Early Miocene to Pliocene), (d) *Calcidiscus pelagicus*, (e) *Calcidiscus leptoporus* (Early Miocene to Pleistocene), (f) *Coccolithus sp.*, (g) *Calcidiscus pelagicus* (Paleocene to Recent), (h) *Umbilicosphaera sibogae* (Middle Miocene to Pleistocene), (i) *Helicosphaera sp.*, (j) *Calcidiscus sp.*, (k) *Reticulofenestra sp.*, (l) *Calcidiscus pelagicus*.

TABLE 1 Summary of onshore reef terrace at Tambolaka.

Reef terrace	Elevation (m)	Width (m)	Lateral correlation at Cape Laundi		
			Elevation (m)	Terraces	Age
T1	8–10	∼200	—	—	—
T2	18–20	∼400	60	II$_1$	MIS 5e
T3	28–34	∼1000	105	II$_5$	MIS 7e
T4	43–46	>100	—	—	—
T5	50–57	∼1000	165	III	MIS 9e
T6	57–60	∼1500	—	—	—
T7	68–72	∼500	210–230	IV	MIS 11c

Note: Assessed as lateral correlation with reef terraces at Cape Laundi in northeast Sumba (Pirazzoli et al., 1991, 1993).
Abbreviation: MIS, Marine Isotope Stage.
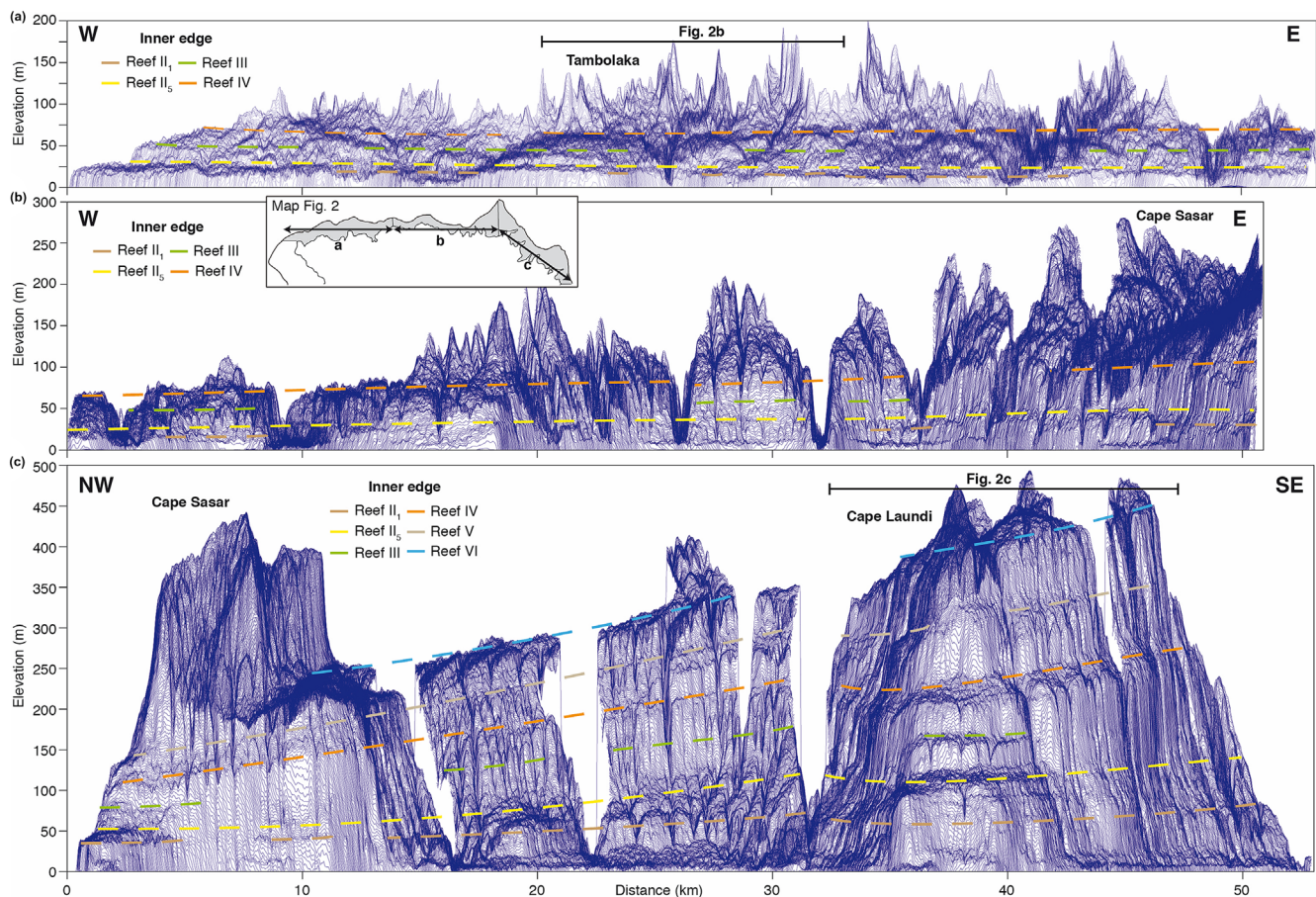
FIGURE 7 Stacked swath profiles of the northwest Sumba coastline. Figure shows a comparison of the coral reef terrace elevations for the area between Tambolaka and Cape Laundi in northwest to northeast Sumba. Areas and viewing directions are given in Figure 2. The elevation shows a significant difference among the four mapped reef terraces with reef elevations decreasing by around 65–75% between Cape Laundi and Tambolaka.

MIS 5e) at Cape Laundi (Chauveau et al., 2023; Pirazzoli et al., 1991, 1993). The third terrace T3 developed at an elevation of ∼28–34 m high and is at least 1 km wide. We propose that this terrace corresponds to terrace II$_5$ (±105 m high; MIS 7e) at Cape Laundi (Figure 7; Chauveau et al., 2023; Pirazzoli et al., 1991, 1993). The fourth terrace T4 is a relatively narrow terrace of a few hundred metres wide, at an elevation of ∼43–46 m. The fifth terrace T5 has a width of ∼1 km and is at an elevation of ∼50–57 m. We propose that this terrace corresponds to Reef III (±165 m high; MIS 9e) at

Cape Laundi (Figure 7; Chauveau et al., 2023; Pirazzoli et al., 1991, 1993). The sixth terrace T6 has a width of ∼1.5 km and lies at an elevation of ∼57–60 m. The seventh terrace T7 has a width of ∼500 m and lies at an elevation of ∼68–72 m. We propose that this terrace corresponds to the distal edge of Reef IV (±210–230 m high; MIS 11c) at Cape Laundi (Figure 7; Chauveau et al., 2023; Pirazzoli et al., 1991, 1993). From diving observations, we found an ∼75 m wide reef with living corals at ∼2 m depth and a second ∼75 m wide reef at ∼6 m depth.

Considering the lateral variations of the mapped reefs (Figure 7), there are clear trends that appear to be similar for Reefs II_1, II_5, III, and IV. Their elevations are relatively high to the SE of Cape Laundi and gradually decrease northwestwards, except for the area just W of Cape Laundi where elevations increase for ~4 km (Figure 7c). Then, elevations decrease by almost half over ~30 km to Cape Sasar and again decrease by almost half for the ~50 km W of Cape Sasar. For the 50 km of coastal stretch around Tambolaka (Figure 7a,b), elevations of the terraces are approximately similar. Whereas Reefs II_5 and IV (T3 and T7 at Tambolaka) are relatively continuous and well-developed, Reefs II_1 and III (T2 and T5 at Tambolaka) are not always clear in morphology.

The mine pit is at ~2.5 km from the coastline, ~2 km E of the cross-section of Figure 2d. Assuming a subhorizontal contact between the Waikabubak and Kalianga Formations (at ~30 masl), we estimate that the open-cut pit would laterally be located below T5, T6, or T7 (Figure 2b). This implies a total thickness of ~20–40 m of Quaternary reefal limestones, which we used as a constraint for reef modelling (next section).

The present-day reef width varies in width between ~100 and ~500 m (Figure 8a), but generally, reefs are a little wider towards Cape Laundi than near Tambolaka. The total reefal terrace width offshore varies more dramatically between Tambolaka and Cape Laundi (Figure 8a), from around 1 km width for the ~100 km W of Cape Sasar but increasing towards ~5 km width at Cape Laundi. The

offshore slopes (Figure 8b) are generally higher around Tambolaka, at around 10–25%, whereas they generally decrease eastward to around 5% at Cape Laundi. Whereas slopes between 130 and 200 m depth and 130–400 m depth are roughly the same for the coastal stretch SE of Cape Sasar, for the coast W of Cape Sasar, the 130–400 m slopes are consistently lower, indicating an overall concave offshore slope. Overall, there is an apparent correlation between the width of the offshore reefal platform and the submarine slope of the island but also with the apparent uplift rate, as indicated by the elevation of the fossil reefs (Figure 8). However, the width of the active reef is seemingly independent of these variables.

4.3 | Reef modelling

We use our modelling results to evaluate the reef morphology and geometry both quantitatively and qualitatively. By exploring the parametric fields, we can infer the conditions under which the observed sequence has been developed. An important metric that our stratigraphic and microfossil analysis provided, which can be directly compared with the reef models, is the full thickness of Quaternary reefs above the mine pit. To achieve Quaternary reef thicknesses of 20–40 m (Figure 9b; see previous section) above elevations of 30 masl, potential reef growth rates have to be 2 mm/year or less, irrespective of the modelled uplift rates, erosion rates, initial slopes,
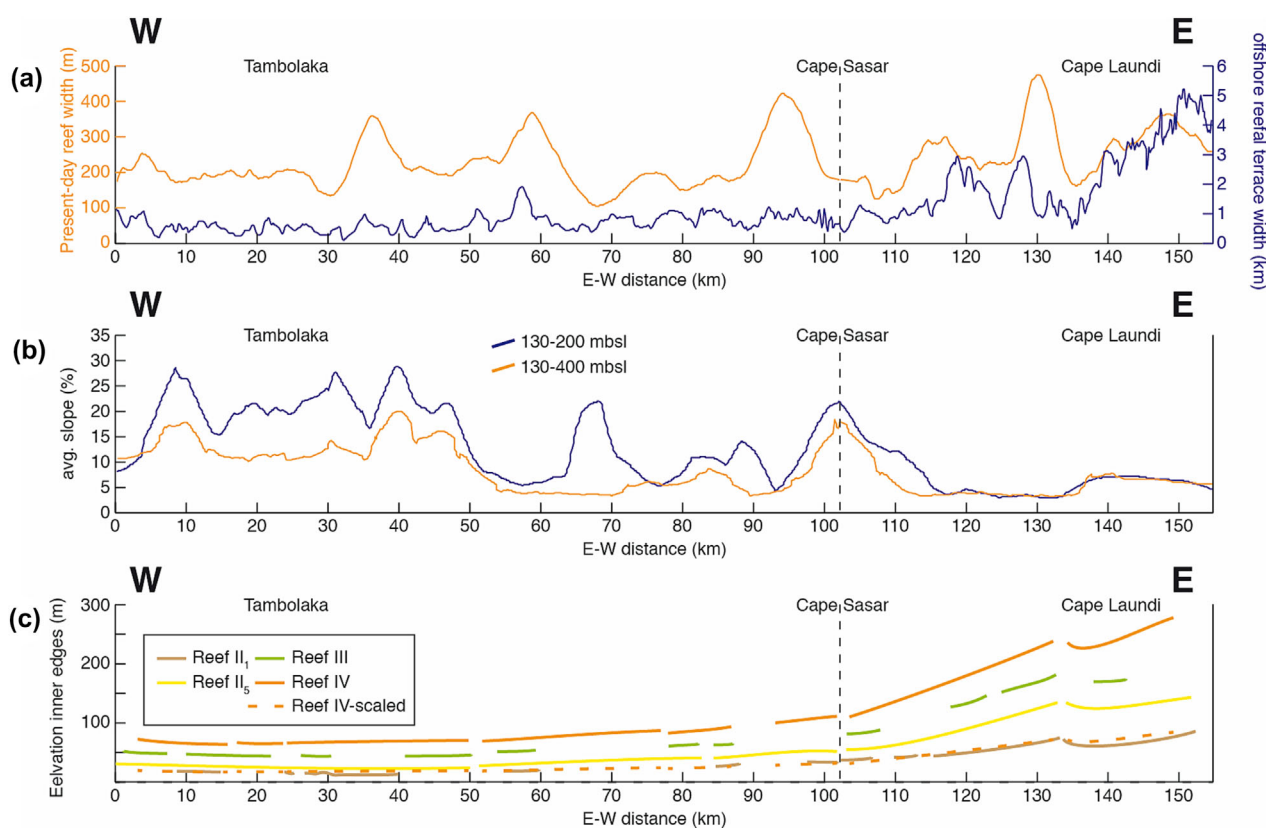
FIGURE 8 Lateral comparison of northwest Sumba coastline. Comparison of several geomorphic reef terrace features between Tambolaka (W) and Cape Laundi (E). (a) Present-day reef width as mapped from Google Earth and offshore reefal terrace width as approximated from the bathymetry (see Section 3). (b) Average offshore slopes for depths of 130 to 200 and 130 to 400 m. (c) Reef terrace elevations for the four main reef terraces that were mapped in the stacked swath profiles of Figure 7. Reef IV-scaled is at a proportion of 122/404 compared with Reef IV: If Reefs II_1 and IV correspond to the MIS 5e (~122 ka) and 11c (~404 ka) highstands, respectively, with constant uplift rates, Reef IV-scaled should be at an approximately similar elevation to Reef II_1.
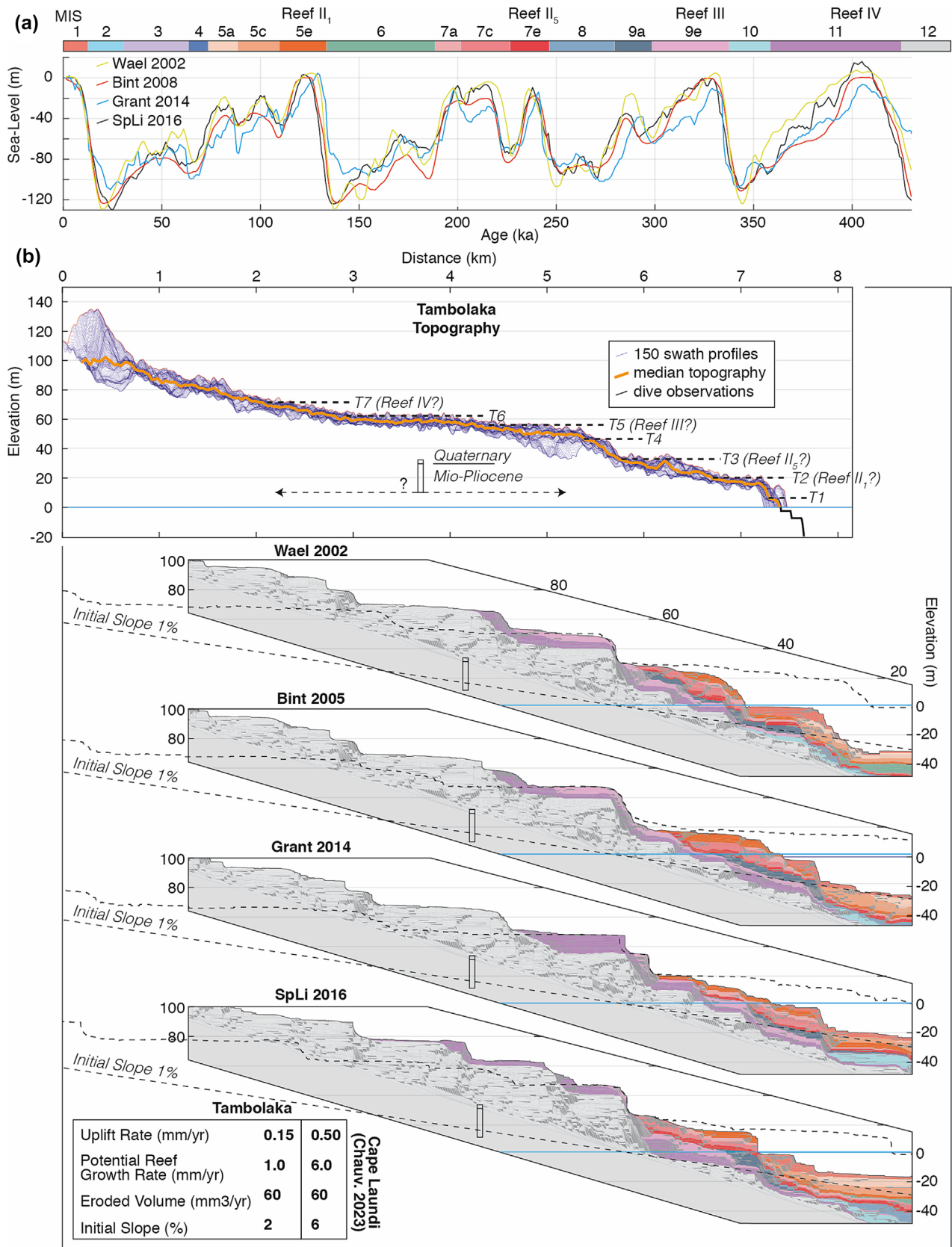
FIGURE 9 Modelling results for the Tambolaka sequence. (a) Sea level curves tested with the model colour codes referring to Marine Isotope Stages (MIS). Wael 2002 = Waelbroeck et al. (2002), Bint 2005 = Bintanja et al. (2005), Grant 2014 = Grant et al. (2014), and SpLi 2016 = Spratt and Lisiecki (2016). (b) Topography of the Tambolaka terrace sequence (same as Figure 2d) for comparison with the models. Models show the full reef architecture for initial slopes of 2%, and dotted lines show the topography and reef base for models with initial slopes of 1%. Model parameters are given in the left bottom inset and compared with the preferred model parameter values for Cape Laundi in Chauveau et al. (2023). Additional model examples are shown in Figure S3.

and sea level curves (Figure 10). The ensemble of modelling results demonstrates that the potential reef growth rate exerts a primary control on the total Quaternary reef thickness, especially for reef growth rates <4 mm/year. For higher rates, the relation between total reef thickness and reef growth is less predictable, and higher potential reef growth rates do not necessarily imply a thicker total reef thickness. Uplift rates of 0.125 mm/year generally imply a thicker reef thickness than rates of 0.15 and 0.175 mm/year, whereas the influence of erosion rate on reef thickness is not very obvious (Figure 10). Although we did not quantify reef thicknesses for the different initial slopes, the examples in Figure 9b show that changing the slope from 2% to 1% mostly changes the reef terrace width, but not the thickness.

Looking at the overall shape of the terrace sequences, the lower part of the sequence from T3 downwards is more consistent with an initial slope of 2%, and the part of the sequence above T3 with wider terraces is more consistent with an initial slope of 1% (dashed lines in Figure 9b). The limited width of the present-day reef that we observed offshore, consistently wider in the models, suggests a higher initial slope percentage offshore. This apparent convex morphology is the opposite of the apparent concave morphology offshore Tambolaka (see previous section). Taking the overall shape

of the terrace sequence, all sea level curves produce a relatively prominent cliff at the inner edge of the MIS 7e terrace, which is consistent with the observed profile and our age interpretation of the Tambolaka terraces. Elevations for this terrace vary per sea level curve, but at elevations of ∼20–30 m, they are comparable with the elevation of the observed T3. In none of the models, there is a big cliff separating MIS 5 and MIS 7 reefs, which is also consistent with the observed profile, where the transition between T2 and T3 is defined by a gentle slope over an elevation change of ∼5 m. All of the models show multiple MIS 5e terraces, of which some are at elevations of ∼8–12 m, similar to the observed T1. Above the MIS 7 terrace, the models show three to four terraces between 40 and 80 m elevation, comparable with the observed T4–T7 terraces in the topography. For this section, the modelled morphology using the Spratt and Lisiecki (2016) curve with a 1% slope matches the observed morphology best: The elevations and locations of the three MIS 9–11 terraces are very similar to the T5–T7 terraces in the Tambolaka sequence. Offshore, the morphology modelled with the Bintanja et al. (2005) and Grant et al. (2014) curves is most similar to the observed two shallow and narrow terraces, showing how two Holocene terraces may have been created during one transgression. In a general sense, it seems terrace elevations are
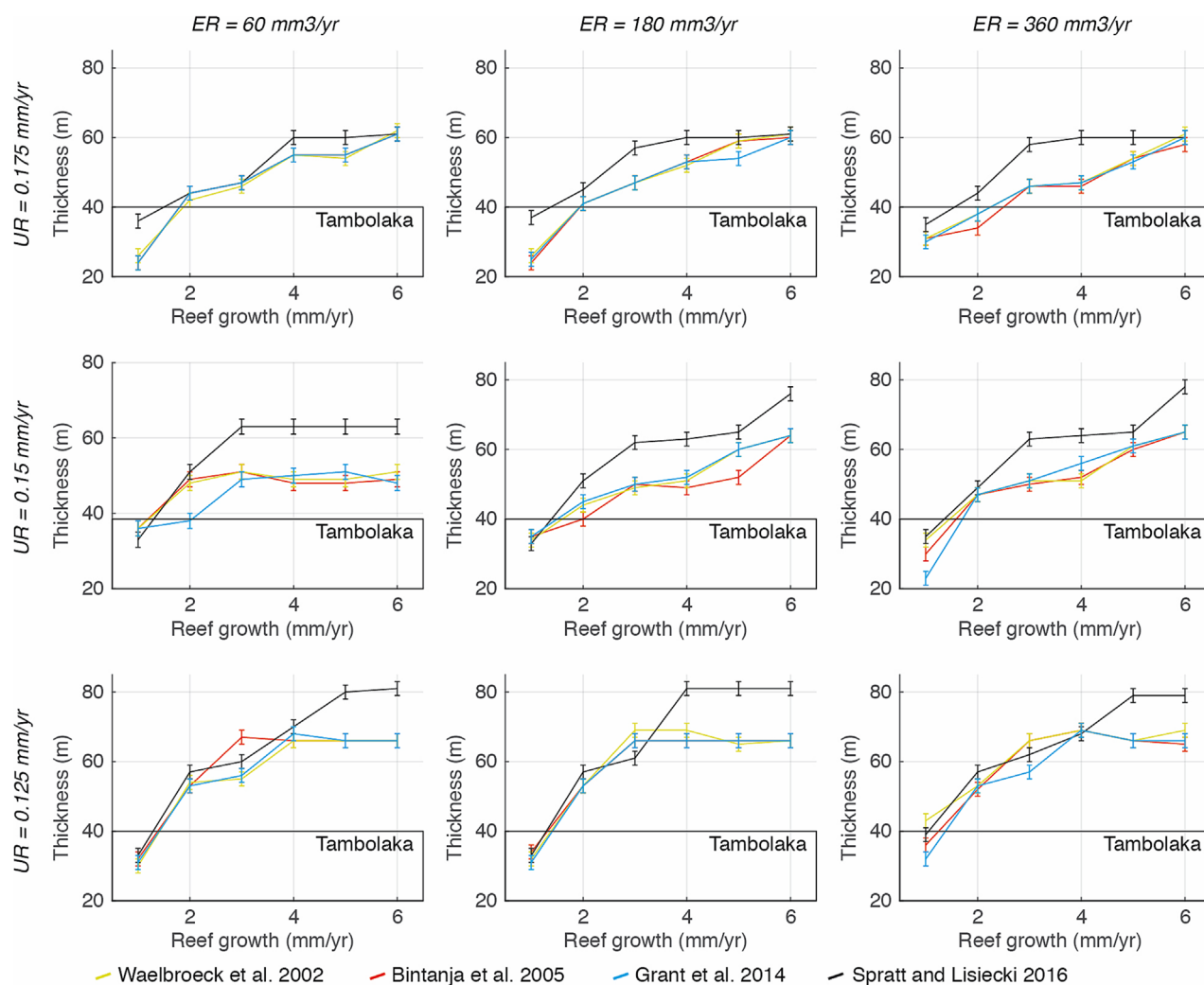
FIGURE 10 Modelled reef thicknesses for different parameters. The stratigraphic and morphologic analysis suggests the full reef thickness at Tambolaka above an elevation of 30 m above sea level is ∼20–40 m, only compatible with potential reef growth rates of 1–2 mm/year. We tested different uplift rates (UR), eroded volumes (ER), and the four sea level curves given in Figure 9a.

mostly controlled by sea level highstands: All the modelled terrace surfaces have ages of either MIS 5, 7, 9, or 11. The width of the terraces seems to rely on the sea level history of the preceding few hundred thousand years, as all modelled terraces were formed over multiple glacial–interglacial cycles given these slow uplift rates.

Figure S3 shows some additional models with different parameters. Changing the erosion rate does not really affect the elevation of the reef terraces nor the reef thickness, but it does change the width of some terraces. The uplift rate does change the elevations and morphology of the terrace sequence (Figure S3). We note that generally, a 0.15 mm/year uplift rate leads to terrace elevations that are more similar to the Tambolaka profile, with the exception of the models with the Grant et al. (2014) curve. In that curve, the MIS 9 and MIS 11 highstands are several metres lower than in the other curves, which may explain why a 0.175 mm/year uplift rate leads to a better match with the observed terraces. Overall, our modelling results demonstrate that uplift rates, initial slopes, and potential reef growth rates at the Tambolaka sequence are all (much) lower than for the Cape Laundi sequence (inset in Figure 9b).

5 | DISCUSSION

5.1 | Stratigraphic correlation

A lithostratigraphic summary of a measured section of the Tambolaka mine pit reveals at least five different reef assemblages. In characteristics, there are considerable distinctions between the four lower layers and the uppermost layer, with the lower units consisting of a bedded chalky limestone unit with a moderately weakly cemented sandy matrix and the top unit consisting of a calcretized reefal limestone with a well-lithified sandy matrix (see Figure 3). The reef framework and facies descriptors are also somewhat different showing matrix-supported floatstone for the four lower layers and grain-supported rudstone for the uppermost layer. In addition, the domal coral-dominated (Faviidae and Poritidae) units identified in the four lower layers (see Figure 4) indicate deeper water environments either below the wave base or in protected areas of the back reef and the lagoon (Wood, 2011).

Based on planktonic foraminifera and nannofossil analyses, the relative age of the reef section in the Tambolaka mine pit confirms earlier observations from a Middle–Late Miocene section in west Sumba (Abdullah et al., 2000). The important species for Late Miocene age in Tambolaka mine pit are *G. plesiotumida* and *G. tumida*. However, the lowermost bedded chalky limestone contained the Oligocene species *G. opima opima*. We suppose that an Oligocene age is too old for the lowermost section in the Tambolaka mine pit (Figure 1), and these species are probably reworked. The chalky limestone was also unlikely to be deposited in a similar period with Oligocene volcanic sediments (Abdullah et al., 2000). Nannofossil analysis was performed to evaluate the age of the lowermost bedded chalky limestone. The most important species discovered in the lowermost section is *U. sibogae*. The species has an age of Middle Miocene to Pleistocene (Bolli et al., 1985). Therefore, combined results of planktonic foraminifera and nannofossil analysis indicate that the age of the Tambolaka mine pit is mostly Middle to Late Miocene and is similar to the section in Lamboya Mountain and

Jawila Mountain (Figure 1; Abdullah et al., 2000). The Quaternary portion of the mine pit section is relatively small, implying that the overall Quaternary thickness around Tambolaka does not exceed 20–40 m.

The carbonate series on Tambolaka in northwest Sumba conforms reasonably well to the Upper Miocene sediment and structure on Central Sumba (Waikabukak Formation; Figure 1), constituting a bedded chalky limestone unit and pelagic marl (Abdullah et al., 2000). Nevertheless, both the carbonate series on Tambolaka and the upper Miocene sediment on Central Sumba contrast with the turbiditic greywacke, tuff, and marly sandstone of Cape Laundi in northeast Sumba. The stratigraphic correlation between west and east Sumba is marked by the interfingering structure between the carbonate series on west Sumba and turbiditic sediments on east Sumba, suggesting that the island tilted eastward during the Miocene (Fortuin et al., 1994, 1997; Satyana & Purwaningsih, 2011b). This observation is explained by the regional geodynamic framework. It is in accord with Fortuin et al. (1994, 1997) who postulated that the Sumba ridge was affected by eastward-increasing subsidence during the Lower Miocene. Overlying the Mio–Pliocene carbonate series on west Sumba and Mio–Pliocene turbiditic sediments on east Sumba, the Quaternary reefal limestones of the Kalianga Formation (Figure 1) are well-preserved on both Tambolaka in northwest Sumba (Authemayou et al., 2022; Nexer et al., 2015) and Cape Laundi in northeast Sumba (Bard et al., 1996; Hantoro, 1992; Jouannic et al., 1988; Pirazzoli et al., 1991, 1993; Rutherford et al., 2001). The collision of the Australian continental plate in the eastern part of the Sunda–Banda islands arc around ∼6 Ma (Haig, 2012) has resulted in a bulldozing effect in the crust of the island arc (Harris et al., 1992) and fast uplift of Sumba. The reefs have been uplifted, resulting in reef terraces along approximately two thirds of the north, west, and east coast of the island (Fleury et al., 2009; Hantoro, 1992; Nexer et al., 2015). Hence, uplift of the Sumba ridge induced by the collision between the Australian plate margin and the Banda arc seems to be relatively young compared with the regional uplift of the outer arc of the Banda Islands (Audley-Charles, 2011; Hall & Smyth, 2008). This is also in agreement with Roep and Fortuin (1996), Harris (2011), and Pirazzoli et al. (1991, 1993) who demonstrated that the beginning of the uplifting process of Sumba ridge was at ∼3 Ma in the east and ∼1 Ma at Cape Laundi. This fast and recent uplift episode is due to tectonic shortening that adds up to the more regional, dynamic uplift of the entire Wallacea caused by the fast reorganization of the underlying subduction dynamics triggered by the collision of the Australian continent (Husson et al., 2022). In addition, Sumba is in the transition between the oceanic subduction and the continental subduction/collision (Figure 1), and the temporal variation of uplift onset age compared with Banda islands is also due to this geodynamic pattern (Authemayou et al., 2022).

5.2 | Reef morphology and modelling

U-series dating of raised coral reefs at Cape Laundi northeast Sumba (Bard et al., 1996; Pirazzoli et al., 1991, 1993) shows that reef terraces along the north coast of Sumba have risen up to ±450 masl at a rate of 0.5–0.65 mm/year since ∼1 Ma. This effect is even more dramatic to the east (Timor), which rises up to ±1700 masl. The dating of a reef cap at 600 masl on nearby Alor (Hantoro et al., 1994) indicates an

uplift of 1.0–1.2 mm/year. Thus, the uplift of that region is, at least locally, twice as fast as in east Sumba.

Hantoro et al. (1995) demonstrated that east Sumba experienced more rapid uplift rates (±0.49 mm/year) than the uplift rate on west Sumba. Nexer et al. (2015) similarly showed that the uplift rates in east Sumba are considerably higher than those on west Sumba, at 0.3–0.6 and <0.3 mm/year, respectively. Our estimate of ∼0.15–0.2 mm/year for Tambolaka, based on a detailed lateral correlation, is compatible with that. Going in more detail, our lateral terrace correlation refines earlier interpretations. The correlation by Nexer et al. (2015) of Reef IV (MIS 11) from Cape Laundi is similar to ours in overall trend but suggests it corresponds to T5 in Tambolaka and not T7 as we propose. Authemayou et al. (2022) proposed a stronger decrease in elevation of the Reef IV terrace from Cape Laundi westward, correlating with T1 or T2 around Tambolaka. We attribute more confidence to our interpretation, as our analysis takes advantage of an 8 m resolution DEM, from which we extracted stacked swath profiles.

We show that the Cape Laundi coral reef terraces that are assigned to the last four major interglacial highstands (MIS 5e, 7e, 9e, and 11c) can be correlated westwards, with their relative elevation differences remaining similar throughout the whole section (Figures 7 and 8). For example, the MIS 5e (∼122 ka; Spratt & Lisiecki, 2016) and MIS 11c (∼404 ka; Spratt & Lisiecki, 2016) sea level highstands were probably at similar elevations (Dyer et al., 2021; Murray-Wallace, 2002) or a few metres higher (e.g., Dutton et al., 2015) compared with present-day sea level. With time-constant uplift rates, the MIS 5e terrace should thus be roughly at elevations of ∼122/404 times the elevation of the MIS 11c terrace. We added a dashed line to Figure 8c that represents such a scaled approximation of Reef IV, and indeed, that line is similar in elevation to Reef II$_1$. This suggests that the Quaternary uplift rate has varied in space but was approximately constant in time over the past ∼400 ka for every given location along the studied coastline. Although we modelled over a longer timescale (1000 ka; see Section 3), morphological analysis for timescales beyond ∼400 ka is hindered by the lack of preserved coral reef terraces at higher elevations (Figure 7).

Apart from the laterally variable uplift rate, the coastal landform is notably different between the two sites, consisting of steep rocky cliff reefal limestone in Tambolaka and gently sloping beach (0–2%) of coarse organic sand with scattered corals in Cape Laundi. Furthermore, the Holocene/present-day reef platform that corresponds to terrace 0 is submerged at Tambolaka but is exposed at Cape Laundi, where it is elevated a few masl, mostly about 75–100 m wide but at some locations attains a width of 150–200 m (Chauveau, Authemayou, Pedoja, et al., 2021; Pirazzoli et al., 1993). Another interesting difference between northeast and northwest Sumba is the variability and difference in slopes. The Tambolaka section onshore suggests a convex morphology with initial slopes of 1–2% between −20 and 100 m elevation (Figure 9), whereas the offshore bathymetry suggests a concave morphology with slopes of 10–25% between −130 and −400 m elevation (Figure 8). In contrast, the onshore and offshore bathymetry in Cape Laundi is surprisingly constant at ∼6% onshore and offshore (Figures 8 and 9). We propose that this is directly related to the structural setting of N-Sumba, as Tambolaka is at the margin of the Sumba Ridge where slopes get steeper towards the NE-Lombok Basin northwards (Figure 1) and then flatten again towards the basin

centre, and Cape Laundi is located more centrally on the ridge. On smaller wavelengths, comparing the mapped folds by Authemayou et al. (2022; Figure 2a) with the stacked swath profiles (Figure 7) suggests the syncline just north of Cape Laundi seems to be subtly expressed in the morphology (Figure 7) of all reef terraces. Conversely, the anticline just south of Cape Sasar is not expressed in the morphology, which suggests that folding there may no longer be active.

A key difference highlighted by the modelling based on the mine pit section is the change in potential reef growth rate between Tambolaka and Cape Laundi, by a factor of 3 to 6. This emphasizes the importance of geodynamic and oceanographic conditions on reef growth, even over distances of ∼100 km, and can serve as a warning to reef modelling studies elsewhere. Generally speaking, many first-order features can be well-reproduced in reef models of Cape Laundi (Chauveau et al., 2023) and Tambolaka (this study). To take a next step in uncovering further details on uplift and relative sea level changes in Sumba, we suggest that future reef modelling work may include the addition of more terrace profiles in the region, as well as a probabilistic assessment of the model parameters.

Our findings indicate that the most prominent highstands do not inherently produce the most prominent coral reef terraces, which is in accordance with Pastier et al. (2019) and Chauveau et al. (2023). For example, in the modelled Tambolaka section, the MIS 7e terrace seems to be persistently better developed than the MIS 5e terrace, even though the latter highstand was higher and lasted longer (Figure 9). In the models, the MIS 7e and 5e terraces grow on top of older reef platforms that started to affect the morphology well before 400 ka (Figure 9), showing how preceding sea level and tectonic history will largely determine the accommodation space available for reefs to grow. In addition, variations in initial basement slope may control the accommodation space for reef growth, as the changes in terrace width at Tambolaka suggest (Figure 9) and as has also been proposed elsewhere (e.g., Cabioch, 2003; Stein et al., 1993). Our models demonstrate that a single highstand can lead to multiple terraces (Figure 9), even if the highstand itself does not consist of multiple peaks (MIS 5 and 11 in this case), which is similar to the findings of Chauveau et al. (2023). As such, these models promote caution in linking coral reef terraces to sea level highstands with a bijective approach (i.e., always linking one terrace to one highstand and vice versa; see discussion in Dumas et al., 2006, and Hearty et al., 2007). A 'dynamic approach' (Pastier et al., 2019) as in this study is a way to allow for a more elaborate consideration of coral reef terrace chronology. As we have demonstrated here, this can be strengthened by analysing different terrace profiles simultaneously and incorporating stratigraphic and geologic findings.

6 | CONCLUSIONS

A transect within the Tambolaka mine pit northwest Sumba shows a bedded chalky limestone unit that contrasts with the turbiditic greywacke, tuff, and marly sandstone of Cape Laundi in northeast Sumba, suggesting different sedimentary environments during the Miocene. Planktonic foraminifera and calcareous nannofossils found in the Tambolaka mine pit indicate a wide range of ages between the Oligocene and Pliocene and support previously proposed eastward tilting of N-Sumba during the Miocene.

Based on morphological observations and reef modelling, we show that, compared with Cape Laundi, Tambolaka has a lower Quaternary uplift rate (~0.15–0.175 mm/year instead of ~0.5 mm/year), narrower present-day reef, lower slopes onshore, higher slopes offshore, and a much lower potential reef growth rate (~1–2 mm/year instead of ~6 mm/year). Based on lateral correlation with stacked swath profiles and supported by reef modelling, we propose a new chronology for the coral reef terraces in northwest Sumba, with seven terraces up to ~70 m elevation spanning the past ~400 ka. Our models show that the most prominent highstand does not necessarily produce the most prominent coral reef terrace, and it is mostly the preceding sea level and tectonic history that will determine the accommodation space available for reefs to grow. This new analysis provides a better understanding of reef stratigraphy and morphodynamics of coral reef sequences, which may serve as a basis to further explore the relative sea level and tectonic history of the island, as well as provide an example for paleo sea level and coral reef terrace studies elsewhere.

AUTHOR CONTRIBUTIONS

ACKNOWLEDGEMENTS

DATA AVAILABILITY STATEMENT

The topographic and bathymetric data used in this study are available for free online (http://tides.big.go.id/DEMNAS and https://tanahair.indonesia.go.id/demnas/#/batnas). The coral reef terrace modelling code is available online (https://github.com/Anne-Morwenn/REEF).

REFERENCES

Abdullah, C., Rampnoux, J.-P., Bellon, H., Maury, R. & Soeria-Atmadja, R. (2000) The evolution of Sumba Island (Indonesia) revisited in the light of new data on the geochronology and geochemistry of the magmatic rocks. *Journal of Asian Earth Sciences*, 18(5), 533–546. Available from: https://doi.org/10.1016/S1367-9120(99)00082-6

Allen Coral Atlas. (2022). Imagery, maps and monitoring of the world's tropical coral reefs. https://doi.org/10.5281/zenodo.3833242

Anderson, R.S., Densmore, A.L. & Ellis, M.A. (1999) The generation and degradation of marine terraces. *Basin Research*, 11(1), 7–19. Available from: https://doi.org/10.1046/j.1365-2117.1999.00085.x

Armijo, R., Lacassin, R., Coudurier-Curveur, A. & Carrizo, D. (2015) Coupled tectonic evolution of Andean orogeny and global climate. *Earth-Science Reviews*, 143, 1–35. Available from: https://doi.org/10.1016/j.earscirev.2015.01.005

Astjario, P. (2006) Akibat ketidakstabilan lereng cekungan dasar laut pada batuan sedimen neogen di desa Kananggar, Kabupaten Sumba Timur, Nusatenggara Timur. *Jurnal Geologi dan Sumberdaya Mineral*, 16(4), 241–250.

Audley-Charles, M.G. (1975) The Sumba fracture: a major discontinuity between eastern and western Indonesia. *Tectonophysics*, 26(3–4), 213–228. Available from: https://doi.org/10.1016/0040-1951(75)90091-8

Audley-Charles, M.G. (2011) Tectonic post-collision processes in Timor. *Geological Society of London, Special Publication*, 355(1), 241–266. Available from: https://doi.org/10.1144/SP355.12

Authemayou, C., Brocard, G., Delcaillau, B., Molliex, S., Pedoja, K., Husson, L., et al. (2018) Unraveling the roles of asymmetric uplift, normal faulting and groundwater flow to drainage rearrangement in an emerging karstic landscape. *Earth Surface Processes and Landforms*, 43(9), 1885–1898. Available from: https://doi.org/10.1002/esp.4363

Authemayou, C., Pedoja, K., Chauveau, D., Husson, L., Brocard, G., Delcaillau, B., et al. (2022) Deformation and uplift at the transition from oceanic to continental subduction, Sumba Island, Indonesia. *Journal of Asian Earth Sciences*, 236, 105316. Available from: https://doi.org/10.1016/j.jseaes.2022.105316

Bard, E., Jouannic, C., Hamelin, B., Pirazzoli, P., Arnold, M., Faure, G., et al. (1996) Pleistocene sea levels and tectonic uplift based on dating of corals from Sumba Island, Indonesia. *Geophysical Research Letters*, 23(12), 1473–1476. Available from: https://doi.org/10.1029/96GL01279

Bintanja, R., Van De Wal, R.S. & Oerlemans, J. (2005) Modelled atmospheric temperatures and global sea levels over the past million years. *Nature*, 437(7055), 125–128. Available from: https://doi.org/10.1038/nature03975

Bock, Y., Prawirodirdjo, L., Genrich, J.F., Stevens, C.W., McCaffrey, R., Subarya, C., et al. (2003) Crustal motion in Indonesia from global positioning system measurements. *Geophysical Research Letters*, 108(B8), 2367. Available from: https://doi.org/10.1029/2001JB000324

Bolli, H.M., Saunders, J.B. & Perch-Nielsen, K. (1985) *Plankton stratigraphy volume 1. Planktic foraminifera, calcareous nannofossils, and calpionellids*. Cambridge: Cambridge University Press.

Bosscher, H., & Schlager, W. (1992) Computer simulation of reef growth. *Sedimentology*, 39(3), 503–512.

Burollet, P., & Salle, C. (1981) A contribution to the geological study of Sumba (Indonesia). *Proceedings Indonesian Petroleum Association. 10th Annual Convention*, 331–344.

Cabioch, G. (2003) Postglacial reef development in the South-West Pacific: case studies from New Caledonia and Vanuatu. *Sedimentary Geology*, 159(1–2), 43–59. Available from: https://doi.org/10.1016/S0037-0738(03)00094-0

Camoin, G.F. & Webster, J.M. (2015) Coral reef response to Quaternary sea-level and environmental changes: state of the science. *Sedimentology*, 62(2), 401–428. Available from: https://doi.org/10.1111/sed.12184

Chappell, J. & Polach, H. (1991) Post-glacial sea-level rise from a coral record at Huon Peninsula, Papua New Guinea. *Nature*, 349(6305), 147–149. Available from: https://doi.org/10.1038/349147a0

Chappell, J. (1974) Geology of coral terraces, Huon Peninsula, New Guinea: a study of Quaternary tectonic movements and sea-level changes. *Geological Society of America Bulletin*, 85(4), 553–570. Available from: https://doi.org/10.1130/0016-7606(1974)85<553:GOCTHP>2.0.CO;2

Chauveau, D., Authemayou, C., Molliex, S., Godard, V., Benedetti, L., Pedoja, K., et al. (2021) Eustatic knickpoint dynamics in an uplifting sequence of coral reef terraces, Sumba Island, Indonesia. *Geomorphology*, 393, 107936. Available from: https://doi.org/10.1016/j.geomorph.2021.107936

Chauveau, D., Authemayou, C., Pedoja, K., Molliex, S., Husson, L., Scholz, D., et al. (2021) On the generation and degradation of emerged coral reef terrace sequences: first cosmogenic 36Cl analysis at Cape Laundi, Sumba Island (Indonesia). *Quaternary Science Reviews*, 269, 107144. Available from: https://doi.org/10.1016/j.quascirev.2021.107144

Chauveau, D., Pastier, A.-M., de Gelder, G., Husson, L., Authemayou, C., Pedoja, K., et al. (2023) Unravelling the morphogenesis of coastal terraces at Cape Laundi (Sumba Island, Indonesia): insights from numerical models. *Preprint*, Available from: https://doi.org/10.31223/X57H48

de Gelder, G., Husson, L., Pastier, A.M., Fernández-Blanco, D., Pico, T., Chauveau, D., et al. (2022) High interstadial sea levels over the past 420ka from the Huon Peninsula, Papua New Guinea. *Communications Earth & Environment*, 3(1), 256. Available from: https://doi.org/10.1038/s43247-022-00583-7

de Gelder, G., Jara-Muñoz, J., Melnick, D., Fernández-Blanco, D., Rouby, H., Pedoja, K., et al. (2020) How do sea-level curves influence modeled marine terrace sequences? *Quaternary Science Reviews*, 229, 106132. Available from: https://doi.org/10.1016/j.quascirev.2019.106132

Dumas, B., Hoang, C.T. & Raffy, J. (2006) Record of MIS 5 sea-level highstands based on U/Th dated coral terraces of Haiti. *Quaternary International*, 145-146, 106–118. Available from: https://doi.org/10.1016/j.quaint.2005.07.010

Dutton, A., Carlson, A.E., Long, A.J., Milne, G.A., Clark, P.U., DeConto, R., et al. (2015) Sea-level rise due to polar ice-sheet mass loss during past warm periods. *Science*, 349(6244), aaa4019. Available from: https://doi.org/10.1126/science.aaa4019

Dyer, B., Austermann, J., D'Andrea, W.J., Creel, R.C., Sandstrom, M.R., Cashman, M., et al. (2021) Sea-level trends across The Bahamas constrain peak last interglacial ice melt. *Proceedings of the National Academy of Sciences*, 118(33), e2026839118. Available from: https://doi.org/10.1073/pnas.2026839118

Effendi, A. & Apandi, C. (1993) Geological map of Sumba quadrangle, Nusa Tenggara Sheet (1:250,000).

Embry, A.F. & Klovan, J.E. (1971) A Late Devonian reef tract on northeastern banks island, N.W.T.1. *Bulletin of Canadian Petroleum Geology*, 19(4), 730–781. Available from: https://doi.org/10.35767/gscpgbull.19.4.730

Fairbanks, R.G. (1989) A 17,000-year glacio-eustatic sea level record: influence of glacial melting rates on the Younger Dryas event and deep ocean circulation. *Nature*, 342(6250), 637–642. Available from: https://doi.org/10.1038/342637a0

Fernández-Blanco, D., de Gelder, G., Lacassin, R. & Armijo, R. (2020) Geometry of flexural uplift by continental rifting in Corinth, Greece. *Tectonics*, 39(1), e2019TC005685. Available from: https://doi.org/10.1029/2019TC005685

Fleury, J.-M., Pubellier, M. & de Urreiztieta, M. (2009) Structural expression of forearc crust uplift due to subducting asperity. *Lithos*, 113(1-2), 318–330. Available from: https://doi.org/10.1016/j.lithos.2009.07.007

Fortuin, A.R., Roep, T.B. & Sumosusastro, P.A. (1994) The Neogene sediments of Eastern Sumba, Indonesia—products of a lost arc? *Journal of Southeast Asian Earth Sciences*, 9(1–2), 67–79. Available from: https://doi.org/10.1016/0743-9547(94)90066-3

Fortuin, A.R., Van der Werff, W. & Wensink, H. (1997) Neogene basin history and paleomagnetism of a rifted and inverted forearc region, on-and offshore Sumba, Eastern Indonesia. *Journal of Asian Earth Sciences*, 15(1), 61–88. Available from: https://doi.org/10.1016/S1367-9120(97)90107-3

Grant, K.M., Rohling, E.J., Ramsey, C.B., Cheng, H., Edwards, R.L., Florindo, F., et al. (2014) Sea-level variability over five glacial cycles. *Nature Communications*, 5(1), 5076. Available from: https://doi.org/10.1038/ncomms6076

Haig, D.W. (2012) Palaeobathymetric gradients across Timor during 5.7–3.3 Ma (latest Miocene–Pliocene) and implications for collision uplift. *Palaeogeography Palaeoclimatology Palaeoecology*, 331-332, 50–59. Available from: https://doi.org/10.1016/j.palaeo.2012.02.032

Hall, R. (2002) Cenozoic geological and plate tectonic evolution of SE Asia and the SW Pacific: computer-based reconstructions, model and animations. *Journal of Asian Earth Sciences*, 20(4), 353–431.

Hall, R. (2012) Late Jurassic–Cenozoic reconstructions of the Indonesian region and the Indian Ocean. *Tectonophysics*, 570, 1–41.

Hall, R. & Smyth, H.R. (2008). Cenozoic arc processes in Indonesia: identification of the key influences on the stratigraphic record in active volcanic arcs, in: special paper 436: formation and applications of the sedimentary record in arc collision zones. Geol. Soc. Am. 27–54.

Hamilton, W. (1979) Tectonics of the Indonesia Region: Geological Survey Professional paper.

Hantoro, W. (1992) Etude des terrasses récifales quaternaires soulevées entre le détroit de la Sonde et l'île de Timor, Indonésie. Mouvements Verticaux de la Croûte terrestre et variations du niveau de la mer, PhD Thesis Univ. d'Aix Marseille II, France.

Hantoro, W.S., Lafont, R., Bieda, S., Handayani, L., Sebowo, E. & Hadiwisastra, S. (1995) Holocene to recent vertical movement in Indonesia: study on emerged coral reef. Proceedings of the International Conference on Geology of South East Asia, 93–113.

Hantoro, W.S., Pirazzoli, P.A., Jouannic, C.H., Faure, C.T., Hoang, U., Radtke, C., et al. (1994) Quaternary uplifted coral reef terraces on Alor Island, East Indonesia. *Coral Reefs*, 13(4), 215–223. Available from: https://doi.org/10.1007/BF00303634

Harris, R. (2011) The nature of the banda arc–continent collision in the timor region. In: *Arc–continent collision*. Berlin, Heidelberg: Springer, pp. 163–211. https://doi.org/10.1007/978-3-540-88558-0_7

Harris, R.A. (1991) Temporal distribution of strain in the active Banda orogen: a reconciliation of rival hypotheses. *Journal of Asian Earth Sciences*, 6(3-4), 373–386. Available from: https://doi.org/10.1016/0743-9547(91)90082-9

Harris, R.A., Wu, S. & Charlton, T.R. (1992) Comment and reply on "Post-collision extension in arc-continent collision zones, eastern Indonesia". *Geology*, 20(1), 92. Available from: https://doi.org/10.1130/0091-7613(1992)020<0092:CAROPE>2.3.CO;2

Hearty, P.J., Neumann, A.C. & O'Leary, M.J. (2007) Comment on "Record of MIS 5 sea-level highstands based on U/Th dated coral terraces of Haiti" by Dumas et al. [Quaternary International 2006 106–118]. *Quaternary International*, 162-163, 205–208. Available from: https://doi.org/10.1016/j.quaint.2006.10.037

Husson, L., Pastier, A.M., Pedoja, K., Elliot, M., Paillard, D., Authemayou, C., et al. (2018) Reef carbonate productivity during quaternary sea level oscillations. *Geochemistry, Geophysics, Geosystems*, 19(4), 1148–1164. Available from: https://doi.org/10.1002/2017GC007335

Husson, L., Riel, N., Aribowo, S., Authemayou, C., de Gelder, G., Kaus, B.J.P., et al. (2022) Slow geodynamics and fast morphotectonics in the far East Tethys. *Geochemistry, Geophysics, Geosystems*, 23(1), e2021GC010167.

Jouannic, C., Hantoro, W.S., Hoang, C.T., Fournier, M., Lafont, R. & Ichram, M.L. (1988) Quaternary raised reef terraces at Cape Laundi, Sumba, Indonesia: geomorphological analysis and first radiometric (Th/U and 14C) age determinations. *Proceedings of the 6th International Coral Reef Symposium*, 441–447.

Koelling, M., Webster, J.M., Camoin, G., Iryu, Y., Bard, E. & Seard, C. (2009) SEALEX—internal reef chronology and virtual drill logs from a spreadsheet-based reef growth model. *Global and Planetary Change*, 66(1–2), 149–159. Available from: https://doi.org/10.1016/j.gloplacha.2008.07.011

Leclerc, F. & Feuillet, N. (2019) Quaternary coral reef complexes as powerful markers of long-term subsidence related to deep processes at subduction zones: insights from Les Saintes (Guadeloupe, French West Indies). *Geosphere*, 15(4), 983–1007. Available from: https://doi.org/10.1130/GES02069.1

Montaggioni, L.F. (2005) History of Indo-Pacific coral reef systems since the last glaciation: development patterns and controlling factors.

Earth-Science Reviews, 71(1–2), 1–75. Available from: https://doi.org/10.1016/j.earscirev.2005.01.002

Murray-Wallace, C.V. (2002) Pleistocene coastal stratigraphy, sea-level highstands and neotectonism of the southern Australian passive continental margin—a review. *Journal of Quaternary Science: Published for the Quaternary Research Association*, 17(5–6), 469–489. Available from: https://doi.org/10.1002/jqs.717

Nexer, M., Authemayou, C., Schildgen, T., Hantoro, W.S., Molliex, S., Delcaillau, B., et al. (2015) Evaluation of morphometric proxies for uplift on sequences of coral reef terraces: a case study from Sumba Island (Indonesia). *Geomorphology*, 241, 145–159. Available from: https://doi.org/10.1016/j.geomorph.2015.03.036

Nienhuis, J. (2019) Local wave and tide data Wavewatch. https://jhnienhuis.users.earthengine.app/view/changing-shores

Nugroho, H., Harris, R., Lestariya, A.W. & Maruf, B. (2009) Plate boundary reorganization in the active Banda arc–continent collision: insights from new GPS measurements. *Tectonophysics*, 479(1–2), 52–65. Available from: https://doi.org/10.1016/j.tecto.2009.01.026

Pacheco, J.F., Sykes, L.R. & Scholz, C.H. (1993) Nature of seismic coupling along simple plate boundaries of the subduction type. *Journal of Geophysical Research - Solid Earth*, 98(B8), 14133–14159. Available from: https://doi.org/10.1029/93JB00349

Pastier, A.M., Husson, L., Pedoja, K., Bézos, A., Authemayou, C., Arias-Ruiz, C., et al. (2019) Genesis and architecture of sequences of Quaternary coral reef terraces: insights from numerical models. *Geochemistry, Geophysics, Geosystems*, 20(8), 4248–4272. Available from: https://doi.org/10.1029/2019GC008239

Peltier, W.R. & Fairbanks, R.G. (2006) Global glacial ice volume and Last Glacial Maximum duration from an extended Barbados sea level record. *Quaternary Science Reviews*, 25(23–24), 3322–3337. Available from: https://doi.org/10.1016/j.quascirev.2006.04.010

Pirazzoli, P.A., Radtke, U., Hantoro, W.S., Jouannic, C., Hoang, C.T., Causse, C., et al. (1991) Quaternary raised coral-reef terraces on Sumba Island, Indonesia. *Science*, 252(5014), 1834–1836. Available from: https://doi.org/10.1126/science.252.5014.1834

Pirazzoli, P.A., Radtke, U., Hantoro, W.S., Jouannic, C., Hoang, C.T., Causse, C., et al. (1993) A one million-year-long sequence of marine terraces on Sumba Island, Indonesia. *Marine Geology*, 109(3–4), 221–236. Available from: https://doi.org/10.1016/0025-3227(93)90062-Z

Rangin, C., Jolivet, L. & Pubellier, M.A.N.U.E.L. (1990) A simple model for the tectonic evolution of southeast Asia and Indonesia region for the past 43 my. *Bulletin de la Soci'et'e g'eologique de France*, 6(6), 889–905.

Roep, T.B. & Fortuin, A.R. (1996) A submarine slide scar and channel filled with slide blocks and megarippled *Globigerina* sands of possible contourite origin from the Pliocene of Sumba Indonesia. *Sedimentary Geology*, 103(1–2), 145–160. Available from: https://doi.org/10.1016/0037-0738(95)00084-4

Rohling, E.J., Grant, K., Bolshaw, M., Roberts, A.P., Siddall, M., Hemleben, C., et al. (2009) Antarctic temperature and global sea level closely coupled over the past five glacial cycles. *Nature Geoscience*, 2(7), 500–504. Available from: https://doi.org/10.1038/ngeo557

Rutherford, E., Burke, K. & Lytwyn, J. (2001) Tectonic history of Sumba Island, Indonesia, since the Late Cretaceous and its rapid escape into the forearc in the Miocene. *Journal of Asian Earth Sciences*, 19(4), 453–479. Available from: https://doi.org/10.1016/S1367-9120(00)00032-8

Satyana, A.H. & Purwaningsih, M.E. (2011a) Multidisciplinary approaches on the origin of Sumba Terrane: regional geology, historical biogeography, linguistic-genetic coevolution and megalithic archeology. *36th HAGI and 40th IAGI Annual Convention and Exhibition*, 1–29.

Satyana, A. H., & Purwaningsih, M. E. (2011b) Sumba area: detached Sundaland terrane and petroleum implications. *Proceedings of Indonesian Petroleum Association, 35th Annual Convention*, 1–32.

Simons, W.J.F., Socquet, A., Vigny, C., Ambrosius, B.A.C., Haji Abu, S., Promthong, C., et al. (2007) A decade of GPS in Southeast Asia: resolving Sundaland motion and boundaries. *Journal of Geophysical Research - Solid Earth*, 112(B6), B06420. Available from: https://doi.org/10.1029/2005JB003868

Soeria-Atmadja, R., Suparka, S., Abdullah, C., Noeradi, D. & Sutanto. (1998) Magmatism in western Indonesia, the trapping of the Sumba Block and the gateways to the east of Sundaland. *Journal of Asian Earth Sciences*, 16(1), 1–12. Available from: https://doi.org/10.1016/S0743-9547(97)00050-0

Spakman, W. & Hall, R. (2010) Surface deformation and slab–mantle interaction during Banda arc subduction rollback. *Nature Geoscience*, 3(8), 562–566. Available from: https://doi.org/10.1038/ngeo917

Spratt, R.M. & Lisiecki, L.E. (2016) A Late Pleistocene sea level stack. *Climate of the Past*, 12(4), 1079–1092. Available from: https://doi.org/10.5194/cp-12-1079-2016

Stein, M., Wasserburg, G.J., Aharon, P., Chen, J.H., Zhu, Z.R., Bloom, A., et al. (1993) TIMS U-series dating and stable isotopes of the last interglacial event in Papua New Guinea. *Geochimica et Cosmochimica Acta*, 57(11), 2541–2554. Available from: https://doi.org/10.1016/0016-7037(93)90416-T

Tate, G.W., McQuarrie, N., van Hinsbergen, D.J.J., Bakker, R.R., Harris, R., Willett, S., et al. (2014) Resolving spatial heterogeneities in exhumation and surface uplift in Timor-Leste: constraints on deformation processes in young orogens. *Tectonics*, 33(6), 1089–1112. Available from: https://doi.org/10.1002/2013TC003436

Taylor, F.W. & Mann, P. (1991) Late Quaternary folding of coral reef terraces, Barbados. *Geology*, 19(2), 103–106. Available from: https://doi.org/10.1130/0091-7613(1991)019<0103:LQFOCR>2.3.CO;2

Tolman, H.L. (2009) User manual and system documentation of WAVEWATCH III TM version 3.14. Technical note, MMAB Contribution, 276(220).

Toomey, M., Ashton, A.D. & Perron, J.T. (2013) Profiles of ocean island coral reefs controlled by sea-level history and carbonate accumulation rates. *Geology*, 41(7), 731–734. Available from: https://doi.org/10.1130/G34109.1

Waelbroeck, C., Labeyrie, L., Michel, E., Duplessy, J.C., McManus, J.F., Lambeck, K., et al. (2002) Sea-level and deep water temperature changes derived from benthic foraminifera isotopic records. *Quaternary Science Reviews*, 21(1–3), 295–305. Available from: https://doi.org/10.1016/S0277-3791(01)00101-9

Wensink, H. & van Bergen, M.J. (1995) The tectonic emplacement of Sumba in the Sunda-Banda arc: paleomagnetic and geochemical evidence from the early Miocene Jawila volcanics. *Tectonophysics*, 250(1–3), 15–30. Available from: https://doi.org/10.1016/0040-1951(95)00048-5

Wood, R. (2011) General evolution of carbonate reefs. In: Hopley, D. (Ed.) *Encyclopedia of modern coral reefs*. Amsterdam: Springer, pp. 452–469. https://doi.org/10.1007/978-90-481-263

Zhang, P., & Miller, M.S. (2021) Seismic imaging of the subducted Australian continental margin beneath Timor and the Banda Arc collision zone. *Geophysical Research Letters*, 48(4), e2020GL089632.

SUPPORTING INFORMATION

Additional supporting information can be found online in the Supporting Information section at the end of this article.

How to cite this article: De Gelder, G., Solihuddin, T., Utami, D.A., Hendrizan, M., Rachmayani, R., Chauveau, D. et al. (2023) Geodynamic control on Pleistocene coral reef development: Insights from northwest Sumba Island (Indonesia). *Earth Surface Processes and Landforms*, 1–18. Available from: https://doi.org/10.1002/esp.5643